

NEUROSCIENCE

Kappa opioids inhibit spinal output neurons to suppress itch

Taylor D. Sheahan^{1*†}, Charles A. Warwick^{1†}, Abby Y. Cui¹, David A. A. Baranger², Vijay J. Perry¹, Kelly M. Smith^{1‡}, Allison P. Manalo¹, Eileen K. Nguyen^{1§}, H. Richard Koerber¹, Sarah E. Ross^{1,3*}

Itch is a protective sensation that drives scratching. Although specific cell types have been proposed to underlie itch, the neural basis for itch remains unclear. Here, we used two-photon Ca^{2+} imaging of the dorsal horn to visualize neuronal populations that are activated by itch-inducing agents. We identify a convergent population of spinal interneurons recruited by diverse itch-causing stimuli that represents a subset of neurons that express the gastrin-releasing peptide receptor (GRPR). Moreover, we find that itch is conveyed to the brain via GRPR-expressing spinal output neurons that target the lateral parabrachial nuclei. We then show that the kappa opioid receptor agonist nalfurafine relieves itch by selectively inhibiting GRPR spinoparabrachial neurons. These experiments provide a population-level view of the spinal neurons that respond to pruritic stimuli, pinpoint the output neurons that convey itch to the brain, and identify the cellular target of kappa opioid receptor agonists for the inhibition of itch.

INTRODUCTION

Itch is an unpleasant sensation that drives organisms to scratch. Itch-inducing stimuli are detected by peripheral sensory neurons that innervate the skin, conveyed to the spinal cord dorsal horn, and finally relayed to the brain where itch can be experienced as a conscious percept. Itch can also be elicited by exogenous application of specific neuropeptides to the spinal cord, including gastrin-releasing peptide (GRP), substance P (SP), and somatostatin (1–9). These pharmacological findings have implicated several spinal neuron populations in itch, including excitatory spinal neurons that express either the gastrin-releasing peptide receptor (GRPR) or neurokinin-1 receptor (NK1R), as well as inhibitory spinal neurons that express the somatostatin receptor (SSTR). However, these receptors are found in different populations of spinal neurons (10, 11), and the manner in which activation of diverse neuron populations elicits the same sensation of itch remains unclear.

A second outstanding question regarding the spinal circuitry that underlies itch is the identity of the spinal output neurons that convey itch input from the spinal cord to the brain. The existence of an itch-specific population of output neurons remains controversial as there is disputing evidence regarding whether spinal output neurons that respond to pruritogens also respond to algogens (12–17). Nevertheless, spinal projection neurons that respond to chemical pruritogens such as histamine are thought to reside within the superficial dorsal horn (primarily lamina I), ascend within the anterolateral tract, and target supraspinal structures including the parabrachial nucleus and thalamus (12, 13, 18, 19). At a molecular level, pruriceptive spinal output neurons have been shown to express *Tacr1*, the gene encoding NK1R (14, 19, 20). However, most spinal output neurons express NK1R (20–22), and thus whether a

subset of NK1R spinal output neurons comprise a pathway for itch requires further investigation.

The number of clinically effective treatments for chronic itch is limited, but kappa opioid receptor (KOR) agonists such as nalfurafine are one of the most effective treatments in humans (23, 24). These drugs similarly reduce itch behavior in mice and monkeys in response to a variety of distinct pruritogens (2, 5, 25–27). Although their site of action remains unclear, the finding that intrathecal delivery of KOR agonists is highly effective in reducing scratching in rodents and monkeys suggests that the spinal cord is a likely target (2, 5, 27). We therefore reasoned that the application of a KOR agonist would reduce the activity in one or more itch-responsive populations in the spinal dorsal horn, which we might be able to identify through population imaging.

Here, we used two-photon (2P) Ca^{2+} imaging to identify a convergent population of spinal neurons that responds to itch-inducing peptides and cutaneous pruritogens. This convergent itch population included only a subset of GRPR interneurons, consistent with growing evidence that GRPR spinal neurons are functionally heterogeneous (28). Unexpectedly, we also found that itch is transmitted to the brain through GRPR-expressing spinoparabrachial neurons (SPBNs), providing evidence that a specific population of spinal output neurons is involved in relaying itch. Further, we show that KOR agonists selectively inhibit GRPR SPBNs to suppress itch. Last, we find that GRPR spinal neurons display cell intrinsic Ca^{2+} oscillations. In sum, our findings reveal the population-level organization of the spinal processing of itch, as well as a cellular target for the inhibition of itch by KOR agonists.

RESULTS

Itch peptides evoke prolonged activity in superficial dorsal horn neurons that parallels scratching behavior

To visualize population-level activity across spinal excitatory neurons in the superficial dorsal horn, we performed 2P Ca^{2+} imaging using an ex vivo spinal cord preparation (Fig. 1A). We used transgenic mice harboring the *Vglut2-ires-Cre* and *Rosa-lsl-GCaMP6s* (Ai96) alleles to achieve targeted expression of the Ca^{2+} -sensitive fluorophore GCaMP6s in excitatory neurons (*Vglut2^{Cre}; Rosa^{GCaMP6s}*

Copyright © 2024 The Authors, some rights reserved; exclusive licensee American Association for the Advancement of Science. No claim to original U.S. Government Works. Distributed under a Creative Commons Attribution NonCommercial License 4.0 (CC BY-NC).

¹Pittsburgh Center for Pain Research and Department of Neurobiology, University of Pittsburgh, Pittsburgh, PA, USA. ²Department of Psychological and Brain Sciences, Washington University in St. Louis, St. Louis, MO, USA. ³Department of Anesthesiology, University of Pittsburgh, Pittsburgh, PA, USA.

*Corresponding author. Email: taylor.sheahan@pitt.edu (T.D.S.); saross@pitt.edu (S.E.R.)

†These authors contributed equally to this work.

‡Present address: Biohaven Pharmaceuticals LTD, Pittsburgh, PA 15203, USA.

§Present address: Department of Anesthesiology and Perioperative Care, University of California, Los Angeles, Los Angeles, CA 90095, USA.

mice). The red fluorescent dye, DiI, was injected into the lateral parabrachial nucleus (IPBN), allowing us to identify spinal projection neurons (Fig. 1, B and C). In these experiments, we recorded the activity of excitatory interneurons and DiI-labeled SPBNs across five optical planes (ranging from 0 to 60 μm from the surface of the gray matter) to capture the activity of neurons in lamina I and II (Fig. 1D).

GRP, somatostatin (or its analog octreotide), and SP are three neuropeptides that cause scratching when delivered intrathecally (1–9). We therefore sought to visualize the activity of spinal excitatory neurons that is evoked by the application of these itch-inducing peptides (Fig. 1, E to P). We anticipated that GRP would directly activate excitatory neurons because GRPR is a G_q -coupled receptor that is predominantly expressed in excitatory superficial dorsal horn neurons, representing ~17% of these neurons (4, 10, 28–31). In response to bath application of GRP to the spinal cord, we observed activity in ~60% of excitatory interneurons in the superficial dorsal horn that lasted for at least 20 min (Fig. 1, E and F and I and J, and fig. S1A). We reasoned that this widespread activity was the result of network activity, i.e., the combination of GRPR neurons responding directly to GRP as well as the neurons that are activated downstream of GRPR neuron activity. Application of octreotide likewise gave rise to prolonged activity, which was observed in 33% of excitatory interneurons (Fig. 1, G and K, and fig. S1B). Because SSTRs are G_i -coupled and they are largely restricted to inhibitory spinal neurons (11, 32, 33), the observed activity in excitatory neurons in response to octreotide application is likely indirect, through a mechanism of disinhibition (e.g., downstream activity; Fig. 1E). Similar to GRP, the application of SP could elicit activity in neurons that express NK1R (a G_q -coupled receptor), as well as those activated downstream of NK1R neuron activity (Fig. 1E). However, in contrast to GRP, SP activated only 6% of excitatory interneurons, and this activity was brief, lasting ~5 min (Fig. 1, H and L, and fig. S1C), consistent with previous work showing that NK1R is rapidly internalized upon activation (34, 35). We then evaluated SPBN activity in response to GRP, octreotide, and SP (Fig. 1M). For each peptide, the overall time course of activity in spinal output neurons was broadly similar to the time course of activity observed in excitatory interneurons (Fig. 1, N to P, and fig. S1, D to F).

Because the sensation of itch elicits scratching, we next examined whether the duration of activity in spinal excitatory interneurons and projection neurons was consistent with the duration of peptide-evoked scratching. Wild-type mice were injected intrathecally with GRP, octreotide, or SP, and scratch bouts were quantified over time (Fig. 1Q). As predicted, the activity of excitatory superficial dorsal horn neurons observed in 2P Ca^{2+} imaging—in particular within spinal output neurons—studies paralleled scratching evoked by each peptide (Fig. 1, R to T), consistent with the idea that ongoing spinal output neuron activity mediates acute itch behaviors.

Itch neuropeptides engage a convergent spinal neuron population that represents a subset of GRPR neurons

The simplest explanation for the observation that spinal application of GRP, octreotide, or SP gives rise to scratching is that all three peptides activate a convergent population of spinal neurons that is involved in mediating itch. Alternatively, each peptide might elicit itch through the activation of independent neuronal populations (Fig. 2A). To distinguish between these two models, we applied itch-inducing peptides in series to determine whether they

activate common subsets of spinal neurons (Fig. 2B). GRP and SP were applied in both the presence and absence of tetrodotoxin (TTX) to distinguish between direct responders (i.e., those that express the cognate receptor) and downstream responders (i.e., those whose activity is secondary to the response in GRPR neurons or NK1R neurons) (fig. S2A). The activation of SSTR by octreotide, in contrast, only produces activity in downstream (ds) excitatory neurons via disinhibition, which we refer to as SSTR-ds neurons. In these experiments, we recorded from >3000 excitatory neurons, 16% (553 of 3367 neurons) of which were activated by at least one itch-inducing peptide. A variety of response profiles were observed among the recorded neurons, and neurons were categorized on the basis of these responses (Fig. 2C and fig. S2B). For simplicity, we refer to neurons that respond to a given peptide as expressing the corresponding receptor (e.g., GRP-responsive neurons are called GRPR neurons).

A preliminary analysis of these response profiles suggested that a large fraction of SSTR-ds neurons were GRPR neurons or neurons that coexpress GRPR and NK1R (GRPR:NK1R neurons). To examine whether this observation could have occurred by chance, we calculated the theoretical overlap if each itch-inducing peptide activated independent populations and compared this with the observed overlap (Fig. 2, D and E). For instance, the theoretical overlap of GRPR, NK1R, and SSTR-ds populations was 0.1%, whereas the observed overlap was 5.6% (Fig. 2E). For statistical analysis, we performed a mixed-effects log-linear regression to calculate an odds ratio which reflects whether an observed overlap of populations is larger or smaller than would be expected if the populations were independent. These analyses can be considered an extension of the classic chi-squared test to three or more variables and further allow us to adjust for differences between mice. We found that the total overlap of cells responding to all three peptides (i.e., GRPR:NK1R:SSTR-ds population) was significantly larger ($P = 6.76 \times 10^{-79}$) than predicted if each peptide activated independent populations of neurons (Fig. 2, E and F). Dramatic enrichment was also observed in GRPR:NK1R and GRPR:SSTR-ds populations (Fig. 2, E and F). These results support the existence of two GRPR spinal neuron populations: one that is responsive to additional itch-causing peptides, which represent ~26% of total GRPR neurons, and another that is unresponsive to these peptides (Fig. 2G). We similarly observed a convergent population that was downstream of GRPR, NK1R, and SSTR neurons (fig. S3, A and B). The finding that common neurons are activated by all three pruritogenic peptides strongly suggests that this convergent population is involved in encoding itch. This convergent population is composed of a subset of GRPR neurons, as well as a common population of neurons that is activated downstream of GRPR itch peptide-responsive neurons.

A subset of GRPR neurons encode responses to both cutaneous pruritogens and spinally acting peptides

Our next goal was to visualize the neurons that are activated in response to cutaneous itch and to determine whether pruritic input from the skin activates the same convergent population of spinal excitatory neurons that was activated by spinally applied peptides. For these experiments, we used intradermal compound 48/80 as a model of urticaria (hives) (36), a condition that is caused by the degranulation of cutaneous mast cells and the release of a variety of endogenous pruritogens including histamine, serotonin, and proteases. To visualize the spinal neurons that respond to intradermal

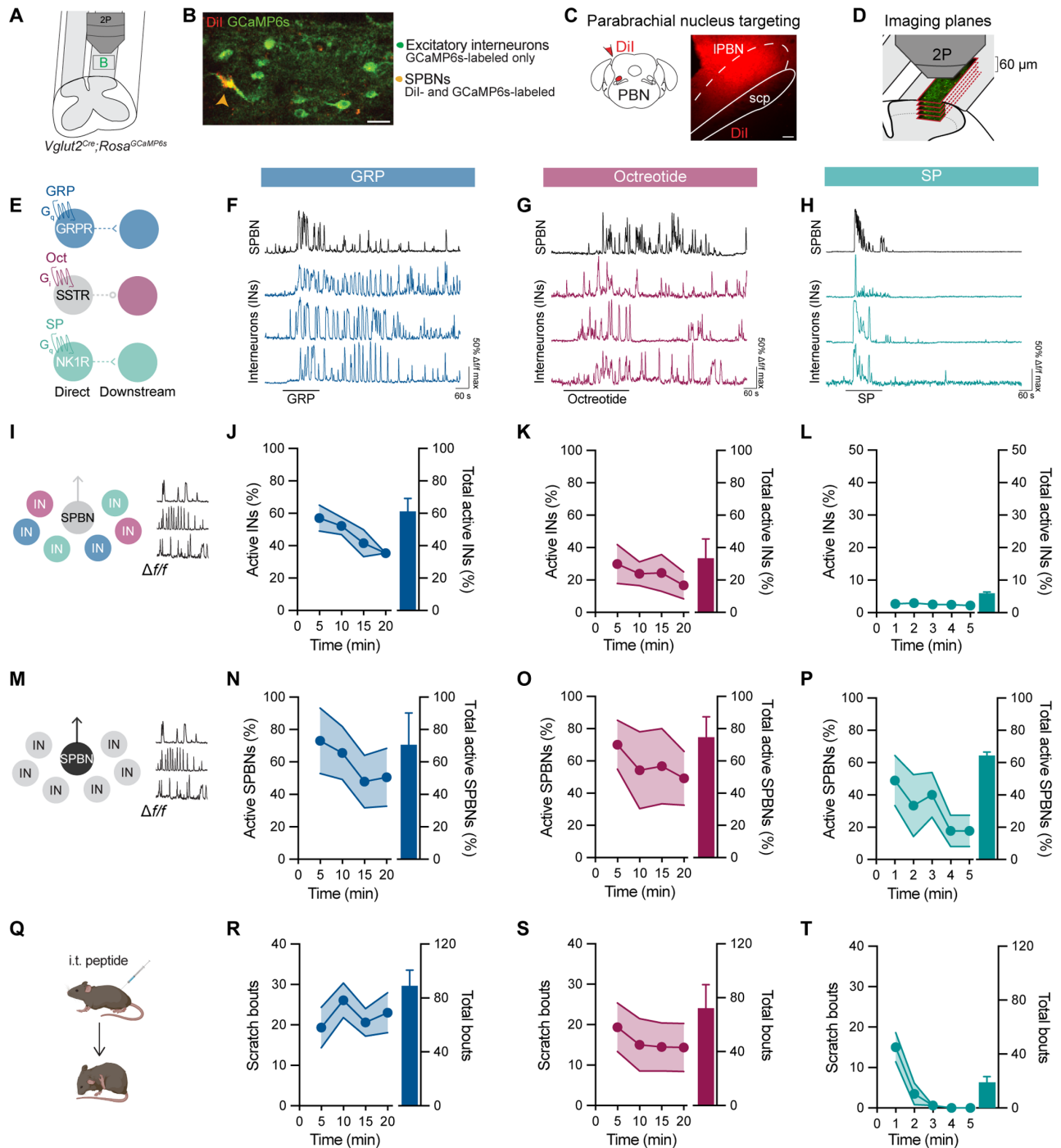


Fig. 1. Neuropeptides evoke prolonged activity in spinal neurons that parallels itch behavior. (A) Strategy to visualize the activity of excitatory spinal cord dorsal horn neurons with GCaMP6s. (B) Labeled excitatory interneurons (INs) and Dil-backlabeled SPBNs (arrowhead). Scale bar, 25 μm . (C) Targeting of the IPBN with Dil. Scale bar, 50 μm . (D) Neurons throughout lamina I and II were imaged across five separate optical planes. (E) Direct and downstream populations activated in response to application of itch-inducing peptides. (F-H) Ca^{2+} traces from interneurons and SPBNs showing network level responses to (F) GRP, (G) octreotide, or (H) SP. (I) Ca^{2+} activity of excitatory INs was analyzed in (J) to (L). (J-L) Percentage of excitatory INs active over time (left y axis) and total percentage of INs activated (right y axis) in response to (J) GRP ($n = 213$ to 596 neurons per mouse, $N = 3$ mice), (K) octreotide ($n = 213$ to 596 neurons per mouse, $N = 3$ mice), or (L) SP ($n = 186$ to 450 neurons per mouse, $N = 5$ mice). (M) Ca^{2+} activity of SPBNs was analyzed in (N) to (P). (N-P) Percentage of SPBNs active over time (left y axis) and total percentage of SPBNs activated (right y axis) in response to (N) GRP ($n = 6$ to 14 SPBNs per mouse, $N = 3$ mice), (O) octreotide ($n = 5$ to 14 SPBNs per mouse, $N = 3$ mice), or (P) SP ($n = 1$ to 14 SPBNs per mouse, $N = 3$ mice). (Q) GRP, octreotide, or SP was administered intrathecally, and spontaneous scratching was quantified in 5-min bins (created with BioRender.com). (R-T) Time course of scratching (left y axis) and total scratch bouts (right y axis) elicited by (R) GRP ($N = 15$ mice), (S) octreotide ($N = 8$ mice), or (T) SP ($N = 10$ mice). [(J) to (L)], [(N) to (P)], and [(R) to (T)]: Data are shown as means \pm SEM; error bars are not visible in (L) given the y axis range.

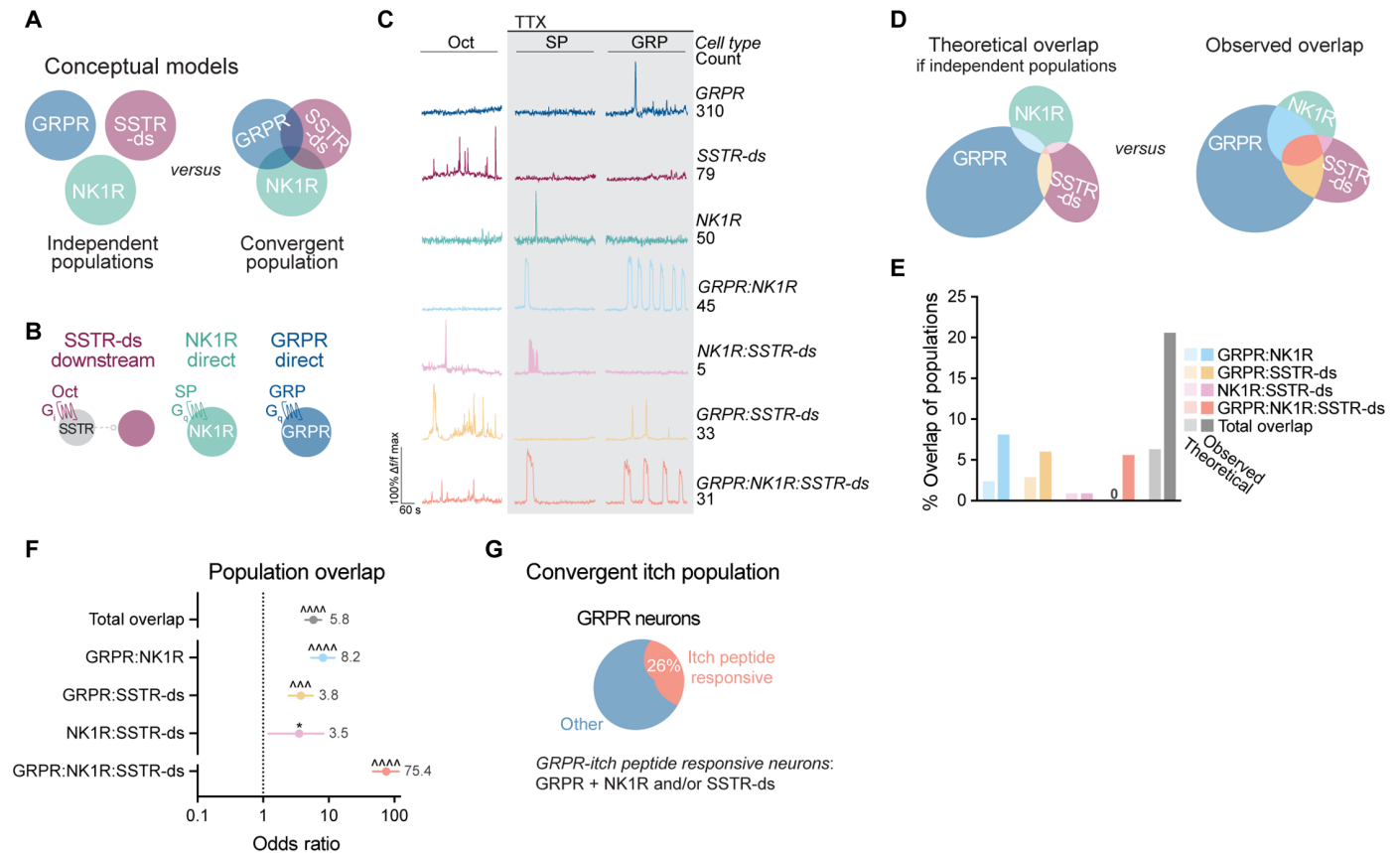


Fig. 2. Diverse itch-causing peptides engage a convergent spinal neuron population. (A) Models for how diverse itch-causing peptides culminate in scratching behavior. Different peptides may engage independent populations (left) or a convergent population of neurons (right). (B) Cell types visualized upon application of octreotide in the absence of TTX (SSTR-ds) and SP or GRP in the presence of TTX (NK1R direct, GRPR direct). (C) Ca²⁺ imaging traces and cell counts of neurons that responded to one or more itch peptides. (D) Extent of population overlap predicted if peptides acted on independent populations of neurons (left) versus the observed overlap of neurons activated by each peptide (right). (E) The percentage of overlap between GRPR, NK1R, and SSTR-ds neurons if they were independent populations (“theoretical”) compared to the observed overlap between populations. (F) GRPR, NK1R, and SSTR-ds populations overlap at frequencies much higher than expected by the prevalence of each cell type ($n = 3367$ total neurons, $n = 236$ to 599 neurons per mouse, $N = 8$ mice). Odds ratio (OR) analyses, Bonferroni correction. OR values for each cell type in gray. Data are shown as odds ratio estimate \pm upper and lower 95% confidence interval (CI). * $P < 0.05$, ^^^ $P < 10^{-8}$, ^^^^^ $P < 10^{-10}$. (G) The convergent itch population of spinal neurons is composed of GRPR neurons that respond to at least one other itch peptide, herein called GRPR itch peptide-responsive neurons. GRPR itch peptide-responsive neurons represent 26% of all GRPR neurons ($n = 109$ of 419 GRPR neurons pooled from $N = 8$ mice).

compound 48/80, we used 2P Ca²⁺ imaging of an ex vivo somatosensory preparation in which the hairy skin of the dorsal hind paw through the proximal hip and corresponding nerves (saphenous and lateral femoral cutaneous) are dissected in continuum from the skin through the dorsal root ganglia and to the intact spinal cord (Fig. 3, A and B). As in earlier experiments, excitatory neurons were visualized using *Vglut2^{Cre}; Rosa^{GCaMP6s}* mice and SPBNs were back labeled with DiI. During imaging sessions, we began by mapping the receptive fields of spinal dorsal horn neurons with punctate mechanical stimuli (Fig. 3C). Thereafter, saline (as a control injection), followed by compound 48/80 were injected intradermally. Once the activity evoked by compound 48/80 waned, we applied octreotide, SP, and GRP to examine whether these itch-inducing peptides activated the same population of neurons as compound 48/80. Last, additional pharmacological profiling was performed to identify cell types based on receptor-mediated responses.

In response to intradermal saline, we observed a brief response (10 to 20 s) in ~50% of excitatory neurons. In contrast, compound

48/80 elicited activity in ~35% of all excitatory superficial dorsal horn neurons, which peaked in 5 min and persisted for at least 30 min (Fig. 3, D to F, and fig. S4A). This was consistent with the duration of compound 48/80-evoked scratching (Fig. 3, G and H). We then used our previously characterized pharmacological cell profiling method (37) to assign molecular identities to the spinal neuron populations that responded to compound 48/80. The ligands used for pharmacological profiling allowed for visualization of neurons that express GRPR, NK3R, TRHR, OXTR, CCKR, NK1R, and CHRM3, thereby enabling the identification of 66% of compound 48/80-responsive neurons (368 of 563 neurons) in lamina I and II (Fig. 3, I to K, and fig. S4B). Among these, the ligand that activated the greatest percentage of compound 48/80-responsive neurons was GRP (Fig. 3K), which comprised 30% of the compound 48/80-responsive cells. Because a single neuron can express multiple receptors (37), we next evaluated which specific receptors were significantly associated with whether a neuron responded to cutaneous injection of compound 48/80. The receptor that was most

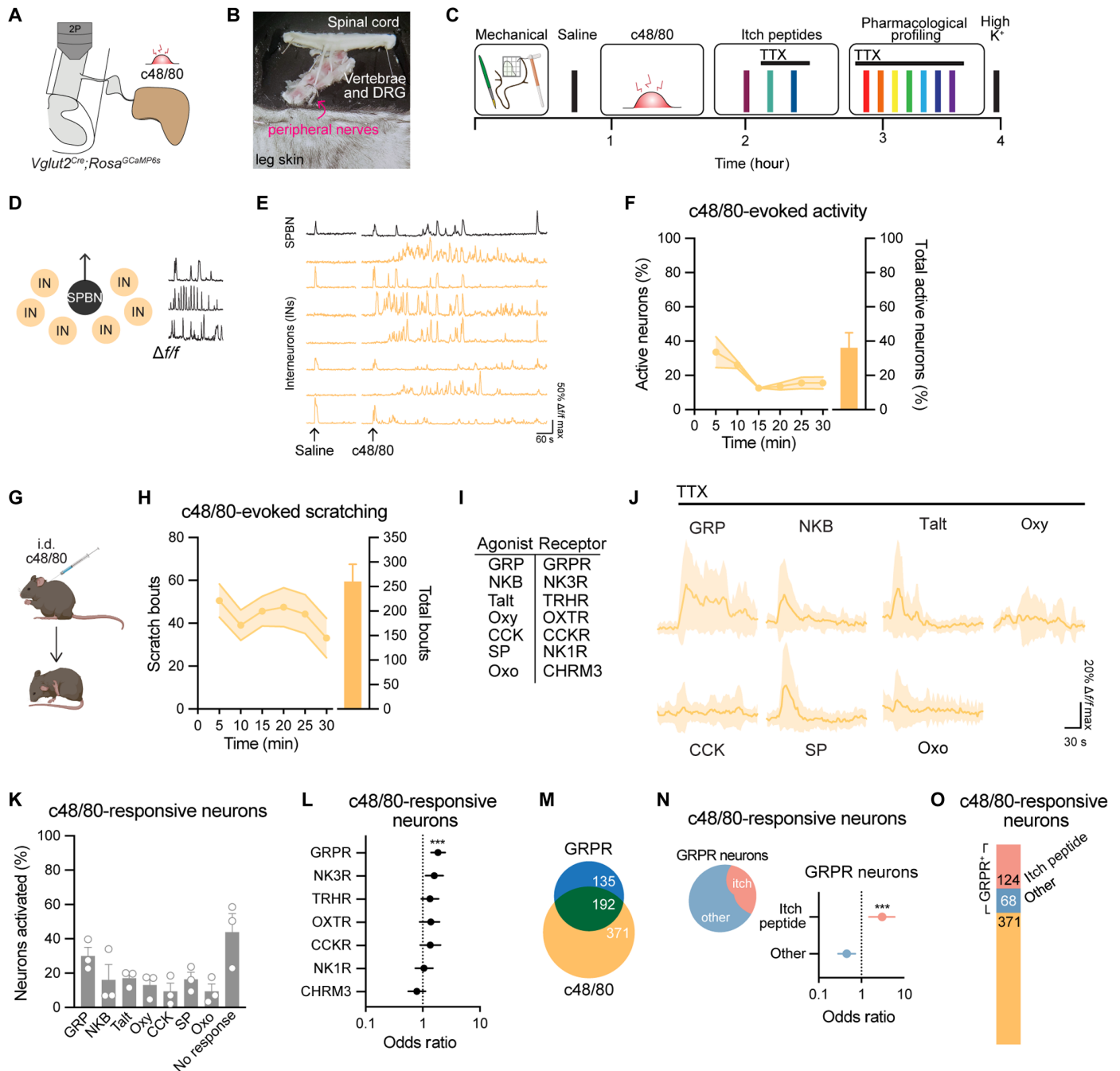


Fig. 3. GRPR spinal neurons encode responses to cutaneous pruritogens. (A and B) Strategy for visualizing excitatory superficial dorsal horn neuron activity evoked by intradermal injection of compound 48/80 (c48/80) using an ex vivo somatosensory preparation. (C) Experimental timeline. (D) Ca^{2+} activity of both INs and SPBNs was analyzed in (E) and (F). (E) Ca^{2+} traces from individual c48/80-responsive neurons. (F) Percentage of neurons activated over time (left y axis) and total percentage of neurons activated in response to c48/80 (right y axis) ($n = 354$ to 610 neurons per mouse, $N = 3$ mice). (G) c48/80 was administered intradermally, and scratching was quantified (created with BioRender.com). (H) Time course of scratching (left y axis) and total scratch bouts (right y axis) following c48/80 injection ($N = 11$ mice). (I) Ligands used to pharmacologically profile neurons and their cognate G_q -coupled receptors. (J) Ca^{2+} responses of c48/80-activated neurons activated by at least one GPCR ligand ($n = 44$ neurons, $N = 1$ mouse). Data are shown as means \pm SD. (K) Percentage of c48/80-responsive neurons activated by GPCR ligands ($n = 87$ to 349 c48/80-responsive neurons per mouse, $N = 3$ mice). (L) GRPR is the only receptor associated with c48/80 responsiveness ($n = 87$ to 349 c48/80-responsive neurons per mouse, $N = 3$ mice). (M) Overlap between GRPR neurons and c48/80-responsive neurons ($N = 3$ mice). (N) GRPR itch-peptide responsive neurons are more likely to respond to c48/80 than other GRPR neurons. (O) Breakdown of c48/80-responsive neurons ($n = 563$ c48/80-responsive neurons pooled from $N = 3$ mice). (F), (H), and (K): Data are shown as means \pm SEM. (L) and (N): Odds ratio analyses, Bonferroni correction where appropriate (L); data are shown as odds ratio estimate \pm upper and lower 95% CI. *** $P < 0.001$.

strongly associated with activity in response to compound 48/80 was GRPR (Fig. 3L and fig. S4C), with GRPR neurons also displaying a greater response magnitude to compound 48/80 compared to neurons lacking GRPR (fig. S4D). Thus, although GRPR neurons are a subset of all compound 48/80-responsive neurons, they represent the cell type that is both most abundant and most responsive among those we visualized.

While GRPR neurons emerged as a key population for the spinal coding of itch, not all GRPR neurons were compound 48/80-responsive; rather, a subset of GRPR neurons responded to compound 48/80 (59%; 192 of 327 GRPR neurons) (Fig. 3M). We therefore analyzed which subset of GRPR spinal neurons responded to compound 48/80 (i.e., GRPR interneurons that also respond to SP and/or octreotide, “GRPR itch neurons,” versus those unresponsive to other itch peptides, “GRPR other neurons”) (Fig. 3N). Just as in the itch-inducing peptides dataset (Fig. 2), the same convergent GRPR itch

peptide-responsive spinal neuron population was present in this compound 48/80 dataset (fig. S5A). Notably, GRPR neurons that responded to additional itch peptides were much more likely to respond to compound 48/80 (Fig. 3, N and O). In sum, these analyses show that peripheral itch input activates the same convergent excitatory spinal neuron population as spinally applied peptides and identify GRPR itch peptide-responsive interneurons as a primary excitatory cell type that responds to compound 48/80.

GRPR spinal projection neurons convey chemical itch to the parabrachial nuclei

To examine how itch information is relayed to the brain, we analyzed which population(s) of SPBNs is activated in response to the cutaneous injection of compound 48/80. Compound 48/80 elicited prolonged activity in 52% of SPBNs (Fig. 4, A to C, and fig. S6A), of which 96% could be categorized by their responses to agonists used for

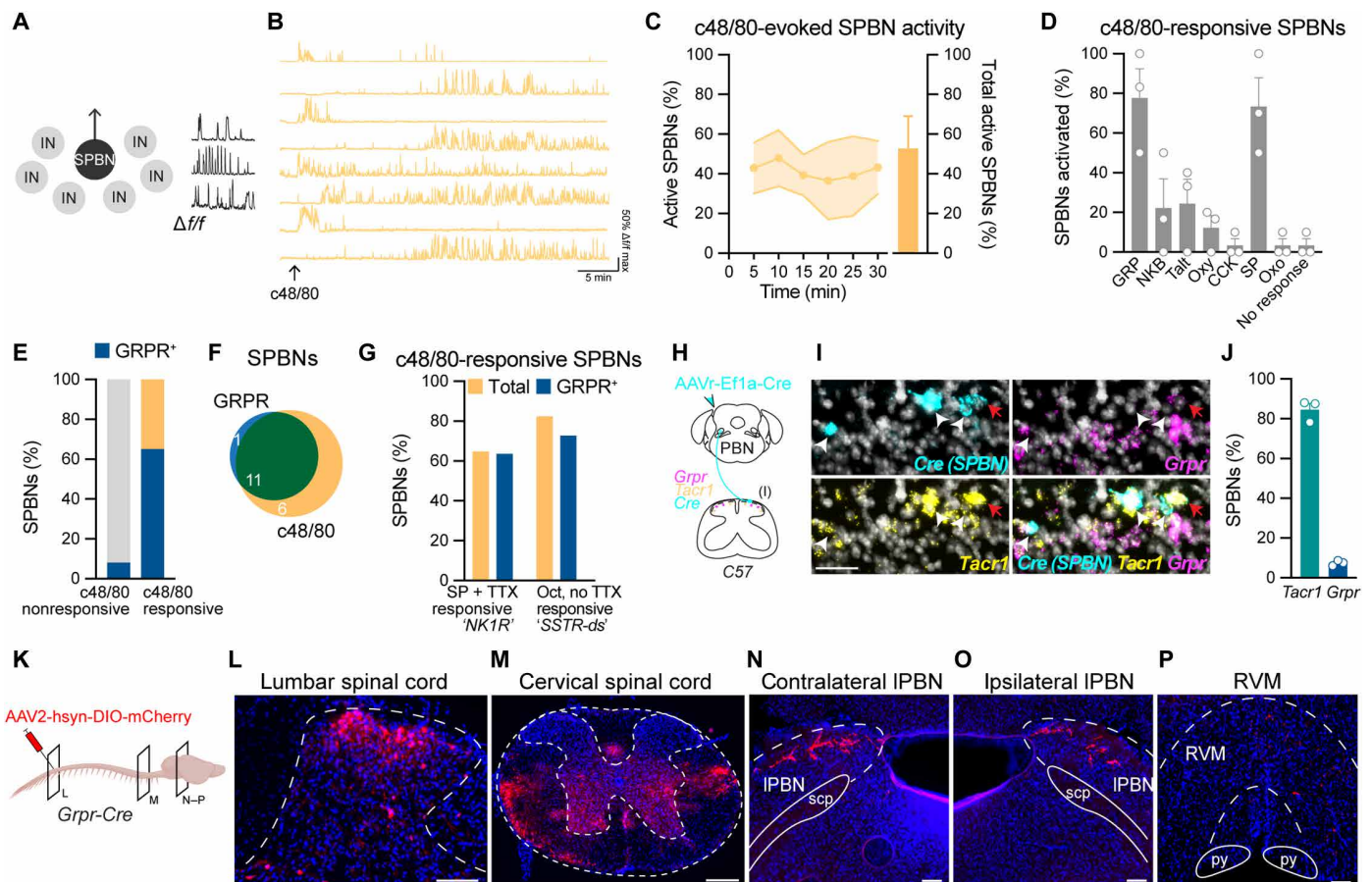


Fig. 4. GRPR SPBNs convey itch to the brain. (A) Ca^{2+} activity of SPBNs was analyzed in (B) and (C). (B) Ca^{2+} traces from individual SPBNs that responded to intradermal injection of c48/80. (C) Percentage of SPBNs activated over time (left y axis), and total percentage of SPBNs activated in response to c48/80 (right y axis) ($n = 5$ to 14 SPBNs per mouse, $N = 3$ mice). (D) Percentage of c48/80-responsive SPBNs activated by ligands used for pharmacological profiling ($n = 1$ to 10 c48/80-responsive SPBNs per mouse, $N = 3$ mice). (E) Percentage of c48/80-responsive and c48/80 nonresponsive SPBNs that express GRPR ($n = 29$ SPBNs pooled from $N = 3$ mice). (F) Overlap between GRPR SPBNs and c48/80-responsive SPBNs (SPBNs pooled from $N = 3$ mice). (G) Most GRPR SPBNs that respond to c48/80 also respond to additional itch peptides ($n = 11$ GRPR⁺ c48/80-responsive SPBNs pooled from $N = 3$ mice). (H) Retrograde labeling of SPBNs for FISH. (I) SPBNs (Cre, white arrowheads) express *Grpr*, *Tacr1*, or both transcripts (red arrows). Scale bar, 50 μm . (J) Percentage of SPBNs that express *Tacr1* versus *Grpr* mRNA. ($n = 23$ to 50 SPBNs per mouse, $N = 3$ mice). (K) Anterograde labeling of GRPR spinal projection neurons to visualize their central projections using *Grpr-Cre* mice (created with BioRender.com). (L and M) *Grpr-Cre* cell bodies at the site of viral injection in the lumbar spinal cord and ascending axons in the cervical spinal cord. Scale bars, 100 and 500 μm , respectively. (N to P) *Grpr-Cre* spinal projection neuron processes target the contralateral IPBN, ipsilateral IPBN, and RVM. Scale bars, 100 μm . (C), (D), and (J): Data are shown as means \pm SEM.

pharmacological profiling (Fig. 4D). To understand the physiological properties—in particular mechanical sensitivity—of compound 48/80-responsive SPBNs, we applied two types of mechanical stimuli to the skin: noxious punctate mechanical input (2.0 g of von Frey filament) and dynamic light brush (Fig. 3C). Together with responses to intradermal injection (i.e., highly noxious input), we used these stimuli to categorize mechanically sensitive SPBNs as high-threshold (HT), low-threshold (LT), or wide dynamic range (WDR) neurons. Compound 48/80-responsive SPBNs accounted for most WDR neurons, although a subset of compound 48/80-responsive SPBNs were also HT and LT responders (fig. S6B).

Strikingly, most compound 48/80-responsive SPBNs responded to GRP in the presence of TTX, indicating that GRPR is expressed in SPBNs. Specifically, 69% of compound 48/80-responsive SPBNs were GRPR SPBNs (Fig. 4E), and 93% of GRPR SPBNs responded to compound 48/80 (Fig. 4F). GRPR SPBNs were HT, LT, and WDR responders and represented ~33 to 50% of each of these mechanically sensitive SPBN populations (fig. S6C). Most GRPR SPBNs were also activated by additional itch peptides (Fig. 4G). The proportion of GRPR SPBNs that responded to compound 48/80 was significantly higher than expected by chance (fig. S6D). In contrast, although many NK1R neurons were found among compound 48/80-responsive SPBNs, this proportion was not higher than expected (fig. S6D), consistent with previous evidence that most SPBNs are activated by SP (38). Together, these data suggest that GRPR SPBNs underlie the transmission of itch input to the brain.

The observation that GRPR is expressed in SPBNs was unexpected as previous evidence suggested that GRPR is exclusively expressed in spinal interneurons (30, 39). To further explore the possibility that GRPR is expressed in spinal output neurons, we performed fluorescent *in situ* hybridization (FISH) on wild-type mice in which SPBNs were retrogradely labeled with virus and probed for expression of *Grpr* (Fig. 4H). As a positive control, sections were costained with *Tacr1*, the gene encoding NK1R, which was detected in 85% of lamina I SPBNs (Fig. 4, I and J, and fig. S6E). *Grpr* was expressed in a subset of SPBNs (~10%), and the majority (75%) of *Grpr* SPBNs coexpressed *Tacr1* (Fig. 4, I and J, and fig. S6E). Consistent with co-expression of GRPR and NK1R at the mRNA level, we analyzed Ca^{2+} responses of SPBNs to GRP and SP in the presence of TTX in an additional dataset. Again, we found strong overlap, with 71% of GRPR SPBNs coexpressing NK1R (fig. S6, F to H). Thus, within the dorsal horn, GRPR expression is not restricted to excitatory interneurons; rather, GRPR is expressed in two distinct populations: excitatory interneurons, as previously described, and lamina I spinal output neurons.

Last, to visualize the central projections of GRPR spinal output neurons, we used *Grpr-Cre* mice and Cre-dependent anterograde labeling through viral expression of AAV2-hsyn-DIO-mCherry in the lumbar spinal cord (Fig. 4, K and L). In these mice, we observed ascending fiber tracts within the anterolateral tract on both the contralateral and ipsilateral sides (Fig. 4M). Within the brain, the most prominent targets of *Grpr-Cre* spinal output neurons were the lateral parabrachial nuclei, which were labeled on both the contralateral and ipsilateral sides (three of three mice analyzed; Fig. 4, N and O). In a subset of mice, sparse mCherry⁺ projections were also observed in the rostral ventral medulla (RVM) (two of three mice analyzed; Fig. 4P). This projection pattern suggests that GRPR spinal output neurons are a subset of lamina I spinal output neurons that bilaterally collateralize to the parabrachial nucleus.

The KOR suppresses itch via selective inhibition of GRPR SPBNs

The kappa agonist nalfurafine is clinically approved in Japan for the treatment of pruritus that accompanies liver or kidney failure (23, 24). Although the specific cell types through which nalfurafine exerts its antipruritic effects remain unknown, the finding that intrathecal nalfurafine reduces numerous types of itch in animal models [e.g., chloroquine- and histamine-evoked itch (5, 40)] suggests the involvement of cells in the spinal cord. Consistent with this, we found that mice pretreated with intrathecal nalfurafine scratched significantly less in response to compound 48/80 and chloroquine compared to mice pretreated with vehicle (Fig. 5, A and B). We next asked whether KOR agonism could block scratching in response to application of itch peptides to the spinal cord. Coadministration of nalfurafine significantly attenuated scratching evoked by direct activation of GRPR, SSTR, or NK1R via intrathecal injection of itch peptides (Fig. 5, C and D). There was no effect of animal sex on KOR inhibition of scratching for any of the itch-causing substances tested (fig. S7, A to D). Together, these results demonstrate that KOR signaling suppresses behavioral responses to both cutaneous pruritogen and spinal itch peptides.

Next, to determine whether KOR is expressed within itch spinal neurons, we performed FISH (Fig. 5, E to I). We found expression of *Oprk1*, the gene encoding KOR, within both excitatory and inhibitory superficial dorsal horn neurons (fig. S8, A and B), consistent with recent RNA sequencing datasets (41, 42). In light of these findings, we reasoned that the simplest mechanism by which KOR signaling could inhibit itch is by suppressing the activity of excitatory superficial dorsal horn neurons. We found *Oprk1* expression in both *Tacr1* and *Grpr* neurons (Fig. 5, E, F, and I). In addition to expression in neurons that express itch neuropeptide receptors, *Oprk1* was also expressed within a subset of neurons that express the itch neuropeptides *Tac1* (SP) and *Grp* (Fig. 5, G to I). Thus, KOR appeared well-positioned to modulate spinal transmission of itch at multiple points within itch spinal circuits, including excitatory interneurons and excitatory spinal projection neurons.

We next sought to pinpoint which spinal neuron populations kappa signaling acts on to suppress itch behavior. Using 2P Ca^{2+} imaging of the *ex vivo* somatosensory preparation, the spinal cord was treated with either artificial cerebrospinal fluid (aCSF) or nalfurafine before intradermal injection of compound 48/80 and activity of excitatory spinal neurons was recorded (Fig. 5J). We first assessed whether nalfurafine had broad effects on interneuron or spinal projection neuron activity. However, the overall activity of interneurons and SPBNs was unchanged by nalfurafine treatment (fig. S9, A and B). Next, on the basis of our population-level analyses, we asked whether KOR agonists acted on the two predominant cell types that respond to itch stimuli: GRPR itch peptide-responsive interneurons and GRPR SPBNs (Fig. 5K). Unexpectedly, nalfurafine reduced the compound 48/80 responses of GRPR SPBNs but not GRPR itch peptide interneurons (Fig. 5, L and M). Further, nalfurafine did not affect the compound 48/80 responses of SPBNs that lack GRPR or other GRPR interneurons (figs. S9, C to E).

Our finding that KOR agonism suppresses the activity of GRPR SPBNs raised the possibility that KOR is expressed in spinal projection neurons. To investigate this, we retrogradely labeled SPBNs with virus and probed for *Oprk1* (Fig. 6A) and found that 55% of SPBNs express *Oprk1* (Fig. 6, B to D). In a subset of mice, we also assessed whether *Oprk1* and *Grpr* are coexpressed in spinal output neurons

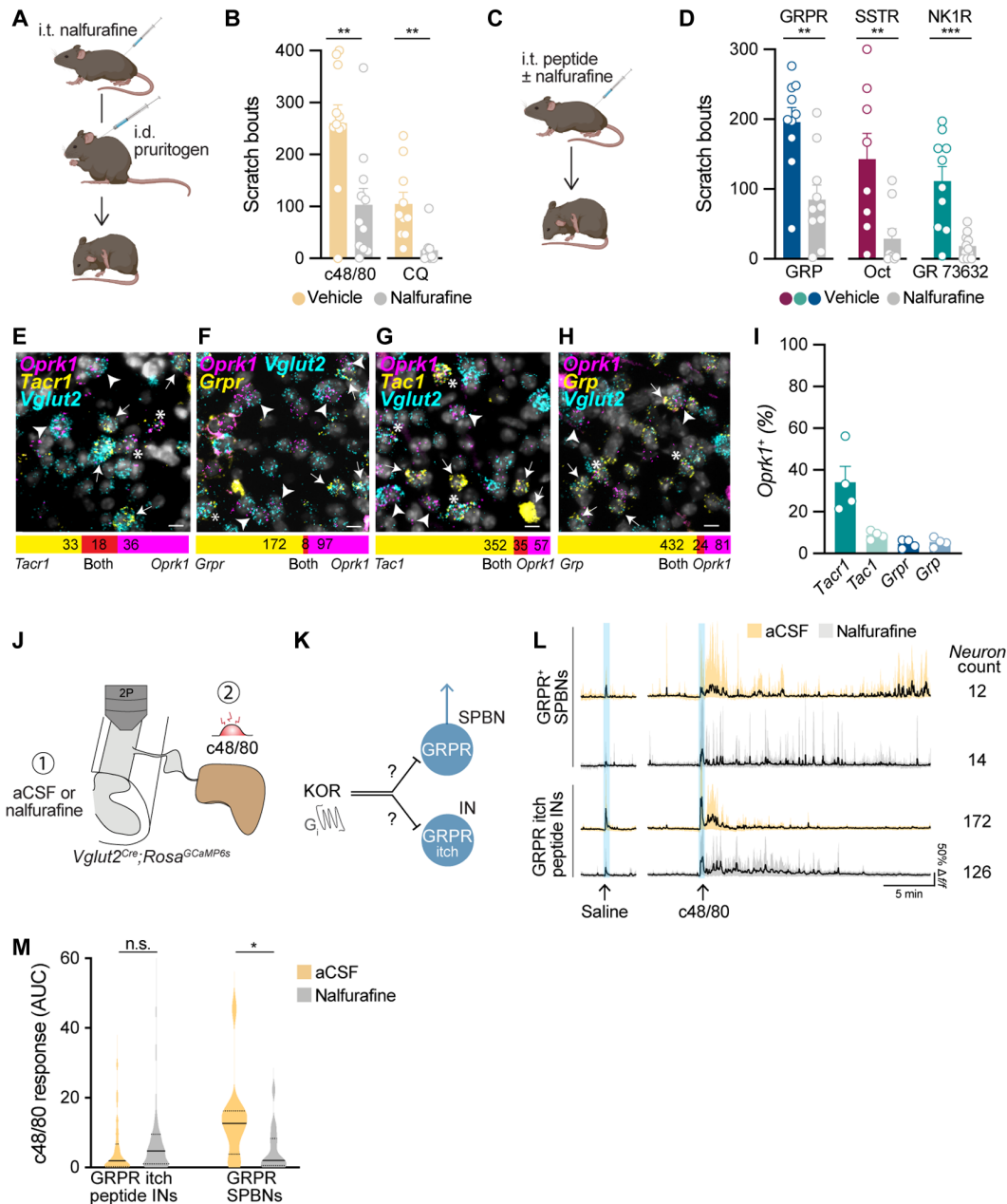


Fig. 5. Kappa opioids suppress itch behavior through inhibition of GRPR SPBNs. (A) Experimental overview (created with BioRender.com). (B) Nalfurafine decreased scratching in response to c48/80 and chloroquine (CQ) ($n = 9$ to 11 mice per group). Student's t test. (C) Experimental overview (created with BioRender.com). (D) Nalfurafine reduced scratching evoked by GRPR, SSTR, and NK1R agonists ($n = 8$ to 11 mice/group). Student's t test. (E to H) Representative images and quantification of excitatory dorsal horn neurons (*Vglut2*) that express *Oprk1* and either (E) *Tacr1*, (F) *Grpr*, (G) *Tac1*, or (H) *Grp*. Scale bar, $10\ \mu\text{m}$. Arrowhead, excitatory *Oprk1* neuron; arrow: *Tacr1*, *Grpr*, *Tac1*, or *Grp* neuron; *triple-labeled neuron. (I) Percentage of *Tacr1*, *Tac1*, *Grpr*, and *Grp* neurons that coexpress *Oprk1*. $N = 4$ mice; neurons per mouse: *Tacr1*: $n = 14$ to 20 , *Tac1*: $n = 13$ to 36 , *Grpr*: $n = 32$ to 57 , *Grp*: $n = 18$ to 36 . (J) Approach for examining the effect of nalfurafine on excitatory spinal neuron activity. (K) Two potential sites of action for KOR inhibition of itch. (L) Ca^{2+} responses of GRPR SPBNs and GRPR itch peptide-responsive INs to c48/80 in the presence of aCSF versus nalfurafine (left) and number of neurons for each subtype/condition (right) (neurons pooled from $N = 3$ to 4 mice per condition). Blue bars, Ca^{2+} transients evoked by intradermal saline. Data shown as means and 10th through 90th percentile. (M) Nalfurafine inhibits Ca^{2+} responses of GRPR SPBNs but not GRPR itch peptide-responsive INs to c48/80 (GRPR⁺ SPBNs: aCSF, $n = 12$ neurons from $N = 3$ mice; nalfurafine, $n = 14$ neurons from $N = 3$ mice. GRPR itch peptide-responsive INs: aCSF, $n = 172$ neurons from $N = 4$ mice; nalfurafine, $n = 126$ neurons from $N = 4$ mice). Linear mixed-effect model, Bonferroni correction. Data shown as median and quartiles. (B) and (D): Data are shown as means \pm SEM. * $P < 0.05$, ** $P < 0.01$, *** $P < 0.001$.

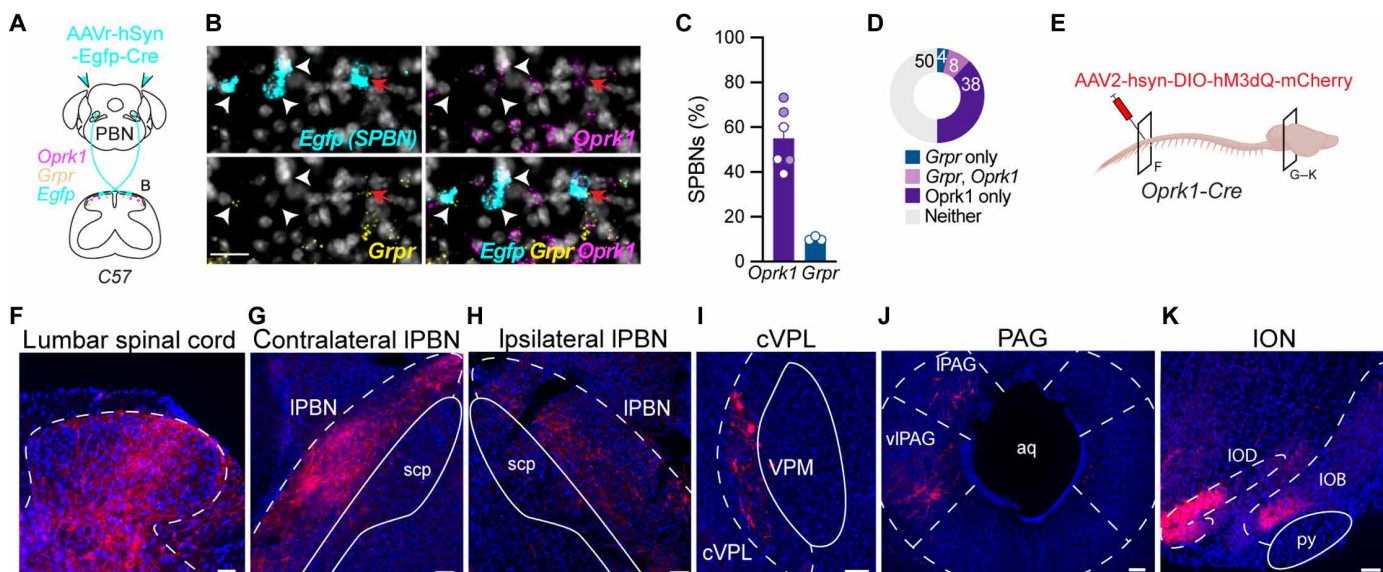


Fig. 6. *Oprk1* and *Grpr* are coexpressed in SPBNs. (A) Retrograde labeling of SPBNs for FISH. (B) SPBNs (*Cre*, white arrowheads) express *Oprk1*, *Grpr*, or both transcripts (red arrows). Scale bar, 25 μ m. (C) Percentage of SPBNs in the superficial dorsal horn that express *Oprk1* or *Grpr*. Shaded circles, experiment probed for *Oprk1* only; white circles, experiment probed for both *Oprk1* and *Grpr* ($n = 19$ to 51 SPBNs per mouse, $N = 3$ mice). Data are shown as means \pm SEM. (D) Most *Grpr* SPBNs coexpress *Oprk1* ($n = 100$ SPBNs pooled from $N = 3$ mice). (E) Anterograde labeling of KOR spinal projection neurons to visualize their central projections using *Oprk1-Cre* mice (created with BioRender.com). (F) Labeling of *Oprk1-Cre* cell bodies at the site of viral injection in the lumbar spinal cord. Scale bar, 50 μ m. (G to K) *Oprk1-Cre* spinal projection neuron processes target the contralateral and ipsilateral IPBN, as well as the contralateral cVPL, PAG, and ION. Scale bars, 100 μ m.

and found that 75% of *Grpr* SPBNs also express *Oprk1* (Fig. 6D). Last, we investigated whether *Oprk1* spinal projection neurons target the same brain structures as *Grpr* spinal projection neurons. We visualized the central projections of *Oprk1* spinal output neurons using *Oprk1-Cre* mice and Cre-dependent anterograde labeling through viral expression of AAV2-hsyn-DIO-hM3dQ-mCherry in the lumbar spinal cord (Fig. 6, E and F). We found that *Oprk1-Cre* spinal output neurons had processes within the contralateral and ipsilateral parabrachial nuclei, consistent with the idea that KOR and GRPR are coexpressed in a subset of bilaterally projecting SPBNs that convey itch to the brain (three of three mice analyzed; Fig. 6, G and H). *Oprk1-Cre*-labeled spinal output neurons likely include additional populations based on their projections to other brain regions, which included the caudal ventral posterior thalamus (cVPL), lateral and ventrolateral periaqueductal gray (PAG), and the inferior olivary nucleus (ION) (three of three mice analyzed; Fig. 6, I to K). Together, these findings suggest that KOR agonists reduce itch through the selective inhibition of GRPR spinal output neurons.

A subset of GRPR spinal neurons display cell-intrinsic Ca^{2+} oscillations

Throughout our Ca^{2+} imaging studies, we noted that in a subset of spinal neurons, GRP elicited a pattern of Ca^{2+} activity that was visually distinct. In these cells, the application of GRP for 3 min gave rise to network-level activity (i.e., both GRPR neurons and neurons activated downstream of GRPR neuron activity) that included repeated Ca^{2+} transients that lasted at least 20 min, and in one experiment, at least 80 min (Fig. 7, A to C, and fig. S10, A to C). To distinguish whether these long-lasting oscillations were a consequence of ongoing circuit activity or whether the oscillations

were a cell-autonomous phenomenon (Fig. 7D), we repeated the GRP application in the presence of TTX. This experiment revealed that GRP-induced oscillations occurred for a similar duration even when network activity was silenced, suggesting that oscillations in GRPR neurons are cell intrinsic (Fig. 7, E to G, and fig. S10, D to F).

To quantify this phenomenon, Ca^{2+} oscillations were defined as three or more Ca^{2+} transients with similar amplitudes that occurred at regular intervals in response to brief application of GRP in the presence of TTX (Fig. 7H). To determine whether cell-intrinsic Ca^{2+} oscillations were specific to GRP, we also tested the effect of other G protein-coupled receptor (GPCR) ligands (Fig. 7I). In addition to GRP, both SP and taltirelin (a thyrotropin-releasing hormone analog) were capable of producing Ca^{2+} oscillations in subsets of excitatory neurons in the dorsal horn; however, GRP was more strongly associated with inducing Ca^{2+} oscillations than any other ligand (Fig. 7J). Specifically, application of GRP gave rise to persistent Ca^{2+} oscillations in $\sim 30\%$ of GRP-responsive cells (Fig. 7I). Because a single neuron can express multiple receptors for these GPCR ligands (37), we then evaluated whether specific cell types were associated with Ca^{2+} oscillations. In the case of SP, neurons that express NK1R were only associated with oscillations if they also expressed GRPR (“GRPR:NK1R”; Fig. 7K); a similar trend was observed for neurons that oscillated in response to taltirelin and expressed TRHR (“GRPR:TRHR”; Fig. 7L). We found that of all of the neurons that displayed cell-intrinsic Ca^{2+} oscillations, GRPR was expressed in 80% of them (197 of 249 neurons, Fig. 7M). Together, these findings show that expression of GRPR is a shared feature of most neurons that oscillate, regardless of which agonist causes oscillations.

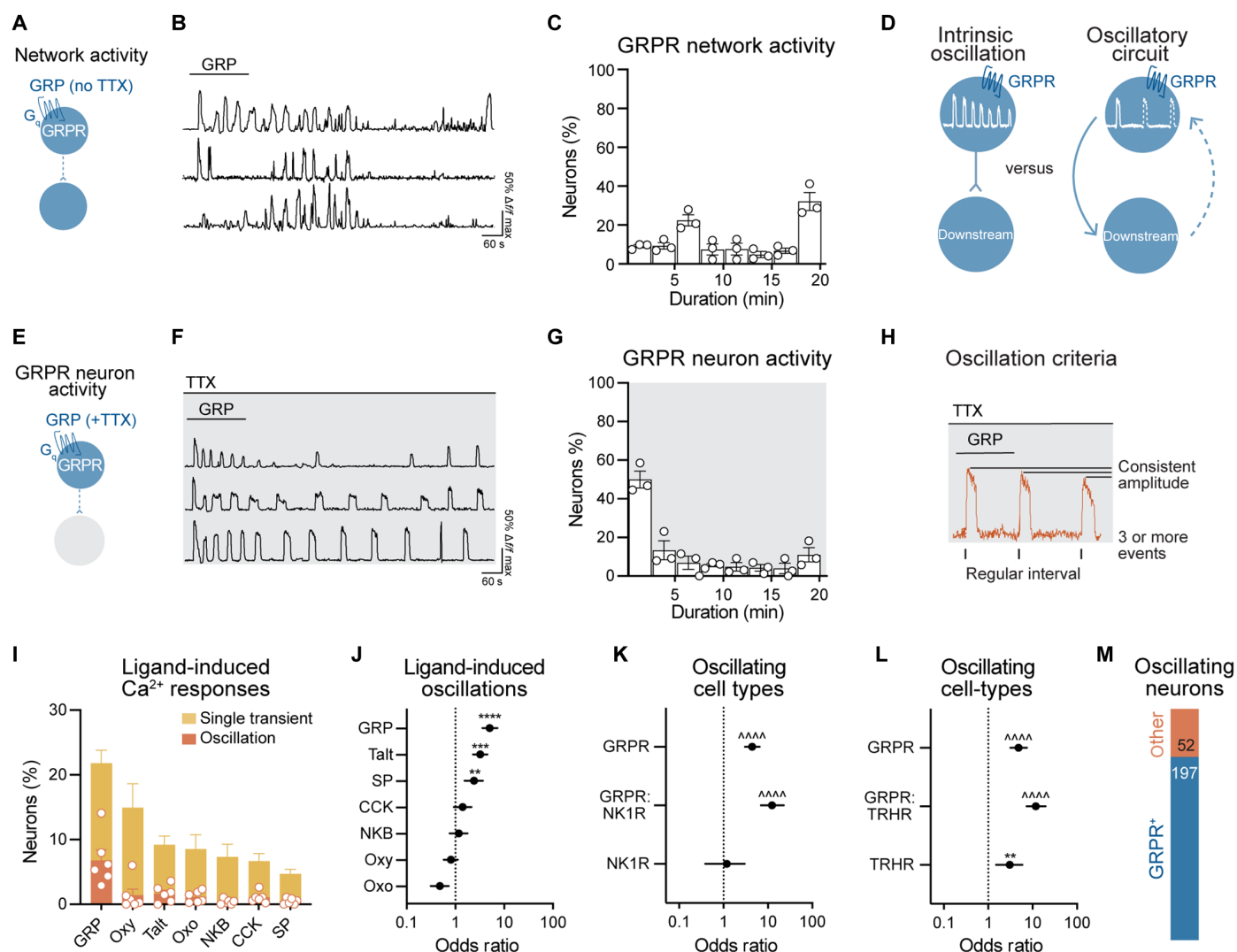


Fig. 7. GRPR neurons can display persistent, cell-intrinsic Ca²⁺ oscillations. (A) Application of GRP in the absence of TTX produces network-level activity in excitatory spinal neurons that express GRPR and those downstream of GRPR neuron activity. (B) Ca²⁺ traces showing GRP-induced Ca²⁺ repeated transients that persist after GRP is washed out. (C) Histogram of the duration of GRP-evoked network activity ($n = 111$ to 447 neurons per mouse, $N = 3$ mice). (D) Models for how oscillations could occur in response to GRP. Oscillations may be an intrinsic feature of GRPR neurons (left) or a consequence of ongoing circuit activity (right). (E) Application of GRP in the presence of TTX produces activity exclusively in neurons that express GRPR. (F) Ca²⁺ traces showing that GRP evokes prolonged oscillations in the presence of TTX. (G) Histogram of the duration of GRP-evoked activity in the presence of TTX ($n = 65$ to 87 neurons per mouse, $N = 3$ mice). (H) Criteria for defining Ca²⁺ oscillations. (I) Percentage of neurons that displayed Ca²⁺ transients versus Ca²⁺ oscillations in response to GPCR ligands applied in the presence of TTX ($n = 275$ to 694 neurons per mouse, $N = 6$ mice). (J) GRP, taltirelin, and SP induce Ca²⁺ oscillations in excitatory spinal neurons ($n = 101$ to 370 ligand-responsive neurons per mouse, $N = 6$ mice). (K and L) GRPR expression is the defining feature of cell types that show cell-intrinsic Ca²⁺ oscillations ($n = 26$ to 66 oscillating neurons per mouse, $N = 6$ mice). (M) Most neurons that display cell-intrinsic Ca²⁺ oscillations express GRPR ($n = 249$ oscillating neurons pooled from $N = 6$ mice). (C), (G), and (I): Data are shown as means \pm SEM. (J) to (L): Odds ratio analyses were performed, with Bonferroni correction where appropriate (J); data are shown as odds ratio estimate \pm upper and lower 95% CI. $**P < 0.01$, $***P < 0.001$, $****P < 0.0001$, $^{\wedge}P < 10^{-10}$.

These findings suggest that a subset of spinal GRPR neurons is notable in their capacity for cell autonomous Ca²⁺ oscillations in response to GRP. The shape and periodicity of these Ca²⁺ oscillations in GRPR neurons were reminiscent of a very well-characterized phenomenon involving cycles of inositol 1,4,5-trisphosphate (IP₃)-mediated Ca²⁺ release and sarcoplasmic reticulum Ca²⁺ ATPase (SERCA)-mediated reuptake (fig. S10G) (43–45). Consistent with this mechanism, we found that GRP-induced Ca²⁺ oscillations were abolished in the

presence of the IP₃ receptor antagonist 2-aminoethoxydiphenyl borate (2-APB) (fig. S10H) and triggered spontaneously in the presence of the SERCA pump inhibitor, cyclopiazonic acid (CPA) (fig. S10I). This type of IP₃-mediated Ca²⁺ oscillation has been extensively characterized in a variety of cell types, such as oocytes, pancreatic acinar cells, and osteoclasts (46–48). Our observations suggest that cell autonomous Ca²⁺ oscillations are also observed in the nervous system, notably in spinal GRPR neurons.

DISCUSSION

In this study, we visualized itch-responsive neurons in the dorsal horn at the population level. We found that itch-causing agents drive spinal neuron activity that parallels the time course of scratching responses and that each itch agent we tested recruited a common population of spinal neurons, which represents a subpopulation of GRPR interneurons. Unexpectedly, we found that most of the spinal output neurons that convey itch to the brain are also GRPR neurons and that these GRPR spinal projection neurons are targeted by the KOR agonist nalfurafine to inhibit itch. Last, we found that GRPR neurons show a distinctive property in that they are capable of persistent Ca^{2+} oscillations.

Population coding of itch

Many studies have investigated the contributions of individual cell types in the dorsal horn to itch, but what has been lacking is a population-level analysis of how itch is encoded. Here, we addressed this fundamental gap in knowledge through 2P Ca^{2+} imaging of the spinal cord dorsal horn. We asked whether three peptides that elicit robust scratching engage a common population of spinal neurons. We found that octreotide acts through disinhibition to drive activity in a population of excitatory neurons that coexpress GRPR and NK1R. These findings are in keeping with and extend the findings of our recent study demonstrating that NK1R is coexpressed within GRPR neurons and that NK1R spinal neurons play a role in itch (4). Moreover, our analyses revealed that convergence continues with a common population of neurons downstream of GRPR, NK1R, and SSTR neurons. Thus, our study provides key insights into the mechanisms by which diverse peptides give rise to itch at the population level. We next visualized the spinal neuron populations that are activated in response to a cutaneous pruritogen and found that compound 48/80 recruits the same subpopulation of GRPR neurons that respond to additional itch peptides. Together, these data reveal that a common population of neurons underlies scratching that occurs in response to a variety of pruritic agents, both cutaneous and spinal.

In combination with our recent work (37), these findings also provide important insights into population coding of pruriceptive versus nociceptive stimuli in the spinal cord. Using the same imaging and pharmacological profiling strategies, we previously delivered the algogen capsaicin into the skin to identify the cell types that underlie allodynia. In contrast to compound 48/80, capsaicin drove activity in neurons that express NK1R/NK3R (Ex_1 neurons), while activity of GRPR neurons (Ex_2 neurons) was largely unchanged. Thus, our findings suggest that, although there is some overlap in the spinal neurons that respond to pruritic and algescic stimuli, the primary cell types that are activated by capsaicin and compound 48/80 are distinct.

GRPR spinal interneurons are heterogeneous

GRPR interneurons have a well-established role in the spinal transmission of itch (1, 3, 4, 20, 49–53). In studies in which GRPR spinal neurons were neurotoxically ablated, itch behaviors were disrupted, while pain behaviors were spared, leading to the idea that GRPR spinal neurons specifically encode itch (49, 52). Our 2P Ca^{2+} imaging studies underscore that GRPR spinal neurons are central to the population coding of itch, as GRP responsiveness is the defining feature of neurons that belong to the convergent itch population, and GRPR functional expression is strongly associated whether excitatory neurons were activated by compound 48/80. However, GRPR

interneurons were not exclusively found within the convergent itch population, nor did all GRPR interneurons respond to injection of compound 48/80, supporting the idea that GRPR interneurons are a functionally diverse population of neurons. This is in keeping with recent evidence that GRPR is expressed in several different populations of spinal interneurons that may have distinct functions, including those that mediate itch, as well as noxious heat and mechanical input (28). Heterogeneity of GRPR neurons is further supported by the detection of *Grpr* in several excitatory dorsal neuron cell types identified in single-cell RNA sequencing analyses (10, 41), as well as their spatial distribution throughout the superficial dorsal horn laminae I–IIo (31, 37, 39, 49). Thus, we propose that there are at least two functional subtypes of GRPR interneurons, of which only one is involved in itch.

This framework also extends to NK1R and SSTR neuron populations, which show a broader laminar distribution throughout the superficial dorsal horn (4, 32, 54), and have been implicated in central sensitization-induced thermal and mechanical hypersensitivity and gating mechanical pain, respectively (55–58). In addition to heterogeneity arising from spatial location within spinal circuitry, our Ca^{2+} imaging findings suggest that spinal neuron subpopulations may differ in their functional expression of peptide receptors. For instance, NK1R is present in both interneurons and spinal projection neurons (4); however, we found that SP predominantly activated SPBNs, in alignment with previous evidence that NK1R is weakly expressed in interneurons (59, 60). In sum, we show that a variety of stimuli that drive scratching do so by recruiting a common population of spinal neurons. Whether this neural organization extends to the manifestation of other aspects of somatosensation is an exciting possibility that merits further investigation.

GRPR neurons show persistent Ca^{2+} oscillations

Neuropeptides have emerged as key molecular mediators of itch throughout the nervous system (61–63). In contrast to neurotransmitters, which can be released at low firing frequencies, the release of neuropeptides tends to require sustained burst firing within neurons (64, 65). In keeping with this, within itch circuitry, pruriceptive primary afferents display bursting activity that is thought to underlie axon reflex, release of CGRP, and erythema (66, 67). Moreover, at the spinal level, burst firing in GRP neurons is required for neuropeptide release and subsequent activation of GRPR spinal neurons (51) and in turn the continued propagation of itch input along the nervous system. In this study, we report that a subset of GRPR spinal dorsal horn neurons show recurrent Ca^{2+} oscillations. As elevated Ca^{2+} is required for burst firing (64, 68, 69), one possibility is that these Ca^{2+} oscillations may similarly facilitate bursting and the release of neuropeptides from GRPR spinal neurons.

Spinal output neurons for itch

The spinal output neurons that relay itch to the brain have remained largely enigmatic. Chemical itch stimuli have been shown to activate SPBNs that express *Tacr1* (14, 20); however, this classification encompasses most lamina I spinal output neurons (20–22, 70). Thus, whether a distinct subset of these neurons represents the output channel of itch to the brain was unknown. Here, we found that the vast majority of SPBNs within the superficial dorsal horn that respond to compound 48/80 also respond to GRP, suggesting functional expression of GRPR. Consistent with previous studies of itch-responsive SPBNs (19, 20), these compound 48/80-responsive,

GRPR⁺ spinal projection neurons also respond to SP (e.g., coexpress NK1R), and we further show that they are activated by other itch peptides such as octreotide. The finding that spinal GRPR neurons are composed of both interneurons and spinal output neurons was unexpected as GRPR was believed to be exclusively expressed in interneurons. Future studies that independently examine the necessity of GRPR spinal projection neurons versus GRPR interneurons for the manifestation of itch (e.g., via targeted activation or silencing of each of these populations) will provide key insights into the relative contributions of each cell type to somatosensory behavior.

In support of the unexpected finding that GRP activates spinal projection neurons, here, we provide convergent evidence from FISH studies that *Grpr* mRNA is expressed in SPBNs. We detected *Grpr* in 7 to 10% of all SPBNs. In contrast, in functional imaging studies, we observed that 28 to 41% of all SPBNs express GRPR (i.e., are activated by GRP), raising the possibility of poor mRNA-protein correspondence for this receptor (71, 72). One outstanding question to be addressed in future studies is whether GRP signaling and/or expression of GRPR is necessary for SPBNs to be activated by itch input.

By leveraging anterograde labeling strategies, we further show that *Grpr-Cre* spinal projection neurons predominantly target the contralateral and ipsilateral IPBN. Consistent with this, a previous study using another genetic allele (*Grpr-Cre^{ERT2}*) also reported labeling of GRPR spinal neurons in these brain regions (73). The finding that the spinal projection neurons responsive to chemical itch stimuli appear to specifically target the PBN is particularly interesting when put into the context of the spinal output neurons for mechanical itch, which were recently shown to exclusively target the PBN (19). Together, these findings suggest that the PBN serves as the initial point of processing of both chemical and mechanical itch input within supraspinal circuits.

KOR inhibition of itch

We and others have previously demonstrated that the endogenous KOR ligand dynorphin is expressed within SSTR spinal neurons (2, 5), but which cells are targeted by dynorphin remained unknown. Because KOR is absent from presumed pruriceptive primary afferents (74, 75), we reasoned that KOR in spinal neurons could be targeted by dynorphin to inhibit scratching. Our in situ hybridization studies suggested that *Oprk1* is well-positioned to suppress excitatory spinal neurons that express itch neuropeptides, as well as neuropeptide receptors, including a subset of *Grpr* neurons. In a previously proposed mechanism for KOR inhibition of itch, KOR was reported to be expressed in roughly half of all GRPR neurons and to inhibit GRPR interneurons through noncanonical PKC δ signaling (40). However, to our surprise, we found no effect of the KOR agonist nalfurafine on the compound 48/80–induced activity of GRPR interneurons. Rather, we observed that activation of KOR signaling caused robust inhibition of GRPR SPBN activity. These SPBNs may represent the small subset of GRPR spinal neurons inhibited by KOR agonists reported in recent studies (28, 76).

Our imaging data raised the possibility that KOR is expressed in spinal projection neurons. In keeping with our finding that KOR agonism suppresses the activity of GRPR SPBNs, anterograde labeling studies revealed projection patterns suggesting that GRPR and KOR are coexpressed in a population of spinal output neurons that bilaterally target the lateral parabrachial nuclei. This idea is further supported by our FISH findings showing that *Grpr* SPBNs

also express *Oprk1*. Together, these results provide a mechanism for KOR inhibition of itch in which KOR signaling suppresses the transmission of itch inputs to supraspinal regions. KOR signaling has also been shown to suppress nociceptive behaviors (77). It is possible that KOR agonists similarly suppress these behaviors by inhibiting the activity of additional spinal output neuron populations, such as those that, we found, target the PAG, RVM, and ION.

An updated model for the spinal coding of itch

In summary, this study provides an updated model of the spinal transmission of itch. In this model, a convergent population of interneurons within the superficial dorsal horn that expresses GRPR integrates itch signals that arise from peripheral stimuli, as well as local spinal neuropeptides. On the basis of evidence that GRPR interneurons arborize in lamina I and make synaptic contacts onto SPBNs (28, 39, 73), we propose that GRPR interneurons make direct connections with GRPR SPBNs. Another source of synaptic input onto GRPR SPBNs may be GRP interneurons, which similarly make monosynaptic connections onto GRPR spinal neurons (51). Our evidence shows that inhibition of these SPBNs may underlie spinal KOR inhibition of itch. While we also identified a convergent neuron population downstream of GRPR interneurons that integrates itch inputs, further studies are required to understand where these neurons fit within a model of spinal itch transmission, although one possibility is that they provide additional inputs onto GRPR spinal output neurons to further shape the coding of sensory inputs to the parabrachial nucleus. More broadly, in this study, we shed light on how previously defined spinal cell types are organized at a population level. This approach can be used as a framework in future studies to enable our understanding of the logic of other aspects of spinal somatosensory processing.

MATERIALS AND METHODS

Animals

Animals were cared for in compliance with the National Institutes of Health guidelines, and experiments were approved by the University of Pittsburgh Institutional Animal Care and Use Committee (protocol number 21100045). *Vglut2-Cre* (Jax, #016963), *RCL-GCaMP6s* (“Ai96,” Jax, #028866), *Snap25-2A-GCaMP6s-D* (“*Snap25^{GCaMP6s}*,” Jax, #025111), and *Grpr-Cre* (Jax, #036668) mouse lines were obtained from the Jackson Laboratories. The *Oprk1-Cre* mouse line was previously generated in our laboratory (Jax, #035045) (78). All transgenic mouse lines were maintained on a C57BL/6 background. The C57BL/6 mice were obtained from Charles River (strain 027). Experiments used a combination of male and female mice, and sex was considered as a biological variable when datasets were sufficiently powered to do so. The mice were housed in groups of up to four (males) or five (females) under a 12/12-hour light/dark cycle. Cages were lined with wood chip bedding. Food and water were provided ad libitum, and plastic housing domes were provided for enrichment.

Viruses

The following viruses were used for anterograde and retrograde labeling of SPBNs: AAV2-hsyn-DIO-mCherry (Addgene, #50459-AAV2), AAV2-hsyn-DIO-hM3Dq-mCherry (Addgene, #44361-AAV2), AAVr-Ef1A-Cre (Addgene, #55636-AAVrg), and AAVr-

hSyn-eGFP-Cre (Addgene, #105540-AAVrg). Viruses were delivered into the spinal cord or IPBN undiluted ranging from titers of 8.6×10^{10} to 2.5×10^{13} .

Stereotaxic injection and retrograde labeling of SPBNs

Stereotaxic injections were performed on 3.5- to 5-week-old mice for 2P Ca^{2+} imaging experiments and 7- to 8-week-old mice for FISH experiments. The mice were anesthetized with 4% isoflurane and maintained in a surgical plane of anesthesia at 2% isoflurane. They were then head-fixed in a stereotaxic frame (Kopf, model 942) and prepared for surgery: The head was shaved, ophthalmic eye ointment was applied, local antiseptic (betadine and ethanol) was applied, and a scalpel was used to make an incision and expose the skull. The skull was leveled using cranial sutures as landmarks. A drill bit (Stoelting, 514551) was used to create a burr hole in the skull, and a glass capillary filled with a retrograde tracer was lowered through the hole to the injection site. The parabrachial nucleus was targeted at the following coordinates: anterior-posterior, -5.11 mm; medial-lateral, ± 1.25 mm; dorsal-ventral, ± -3.25 mm (from the surface of the skull). A Nanoinject III (Drummond Scientific, 3-000-207) was used to deliver either 250 to 300 nl of the retrograde tracer Fast DiI oil (2.5 mg/ml) or 500 nl of retrograde viruses at 5 nl/s. The glass capillary was left in place for 5 min following the injection and slowly withdrawn. The scalp was sutured closed with 6-0 vicryl suture. For postoperative care, the mice were injected with ketofen (5 mg/kg) and buprenorphine (0.03 mg/kg) and allowed to recover on a heating pad. Experiments began at least 4 days following DiI injection and at least 5 weeks after viral injection to allow sufficient time for the retrograde label to reach the spinal cord. To verify targeting of retrograde tracers, the brains were collected, postfixed overnight in 4% paraformaldehyde, sunk in sucrose, and sectioned at 60 μm . The sections were checked for fluorescence in the IPBN as mapped in the Allen Mouse Brain Atlas.

Ex vivo preparations

Ex vivo preparations for 2P Ca^{2+} imaging were performed on 5- to 7-week-old mice. All solutions were saturated with 95% O_2 and 5% CO_2 for the duration of the experiment. Sucrose-based aCSF consisted of (in millimolar): 234 sucrose, 2.5 KCl, 0.5 CaCl_2 , 10 MgSO_4 , 1.25 NaH_2PO_4 , 26 NaHCO_3 , and 11 glucose. Normal aCSF solution consisted of (in millimolar): 117 NaCl, 3.6 KCl, 2.5 CaCl_2 , 1.2 MgCl_2 , 1.2 NaH_2PO_4 , 25 NaHCO_3 , 11 glucose. The mice were anesthetized with ketamine (87.5 mg/kg)/xylazine (12.5 mg/kg) cocktail before beginning dissections. After the dissection, the recording chamber was placed in the multiphoton imaging rig, and sucrose-based aCSF was gradually replaced with normal aCSF over 15 min to avoid shocking the tissue. Meanwhile, the temperature of the aCSF was slowly brought from room temperature to 26° to 28°C . Imaging began ~ 45 min following washout of the recording chamber with aCSF to allow time for recovery of the cells, thermal expansion, and settling of the tissue. Dissection details for each preparation follow below.

Ex vivo spinal cord preparation

All itch peptide and GRP-induced oscillations experiments were conducted on *Vglut2^{Cre}*; *Rosa^{GCaMP6s}* mice. The mice were transcardially perfused with chilled, sucrose-based aCSF. The spinal column was dissected out and chilled in sucrose-based aCSF. The ventral surface of the spinal column was removed, and the spinal cord

segment corresponding to the T10 to S1 was carefully removed. Nerve roots were trimmed, and the dura and pia mater were removed. Next, using Minutien pins (FST, catalog: 26002-202), the spinal cord was secured in a Sylgard-lined recording chamber such that the gray matter of the dorsal horn would be parallel with the imaging objective.

Ex vivo semi-intact somatosensory preparation

All compound 48/80 control experiments were conducted on *Vglut2^{Cre}*; *Rosa^{GCaMP6s}* mice. In kappa agonist experiments, four *Vglut2^{Cre}*; *Rosa^{GCaMP6s}* mice and two *Snap25^{GCaMP6s}* mice were used, with only SPBNs included in analyses from *Snap25^{GCaMP6s}* mice. The hind paw, leg, and back were closely shaved, leaving only 2 to 3 mm of hair in place. The mice were transcardially perfused with chilled, sucrose-based aCSF. An incision was made along the midline of the back, and the spinal cord was exposed via dorsal laminectomy. The spinal column, ribs, and leg were excised and transferred to a Sylgard-lined dish and bathed in sucrose-based aCSF. The lateral femoral cutaneous and saphenous nerves were dissected out in continuum from the skin to the dorsal root ganglia. The thoracolumbar spinal cord was carefully removed from the spinal column, keeping the spinal roots intact. Next, the spinal cord was securely pinned with Minutien pins as described above, and the dura mater was removed along the entire length of the spinal cord. The pia mater was removed from the L1–L2 recording area. Last, the nerves and nerve roots were gently loosened from the tissues, and the skin was pinned out as far from the spinal cord as possible, allowing for a light shield to be placed between the skin and objective at the spinal cord during cutaneous injections.

Multiphoton imaging

2P Ca^{2+} imaging was performed on a ThorLabs Bergamo II microscope equipped with an 8-kHz resonant-galvo scan path, GaAsp detectors, a piezo objective scanner for high-speed Z-control during volumetric imaging, and paired with a Leica 20 \times (numerical aperture, 1.0) water immersion lens. A Spectra Physics Mai Tai Ti:Sapphire femtosecond laser tuned to 940 nm was used to excite the fluorophores. Fluorescence was captured with FITC/TRITC emission filter sets with a 570-nm dichroic beam splitter. Five different planes were imaged simultaneously at 8.5 Hz with 15 μm between planes, providing an imaging depth of 0 to 60 μm below the surface of the gray matter. Scanning was performed with a 1.4 \times optical zoom at a 512 by 256 pixel resolution providing a 514 μm -by-257 μm field of view, yielding a pixel resolution of ~ 1 μm per pixel. This volumetric scanning approach allowed simultaneous sampling from lamina I and II and yielded between 250 and 600 excitatory neurons per experiment.

Receptive field mapping and applying mechanical stimuli in the ex vivo semi-intact somatosensory preparation

In experiments evaluating cutaneous itch inputs, receptive field mapping was performed under low magnification to empirically identify the region of gray matter receiving primary afferent input from the skin as described previously (37). Briefly, a wide brush was used as a search stimulus to pinpoint the correct field of view. A wide brush (Somedic, 15 mm-by-5 mm brush) was swept over the entire length of dissected skin, activating as many afferent inputs as possible. Brushing was repeated three times, with 60 s between applications. The imaging region was refined iteratively until the

region with the most change in fluorescence in response to brushing was in the field of view, and the final 1.4× optical zoom was applied. Next, a 2.0-g von Frey filament was applied to the skin to locate the 15 mm-by-15 mm region of skin that received the greatest afferent input, which was marked with a surgical felt tip pen. The filament was applied to each location for 1 s, with 15 s between applications. Imaging, feedback sensors (thermocouples, load cells, etc.), and event times were synchronized using Thorsync.

Intradermal injections in the ex vivo semi-intact somatosensory preparation

Injection of either saline or compound 48/80 (91 μg in 10 μl) was performed with a 31-G needle. The needle was held nearly parallel with the skin, bevel side up, and carefully inserted into the skin. The injections were targeted to the center of the mapped receptive fields and were considered successful if they resulted in a visible bleb. Saline was randomized to be given either before or after compound 48/80, and no significant differences were noted in the response order. We observed that both the saline and compound 48/80 injections gave rise to a brief Ca²⁺ response, likely due to the noxious mechanical distension of the skin. When assessing whether neurons were compound 48/80-responsive, this initial injection response is excluded from analysis. In experiments examining the effect of nalurafine on the responses of excitatory neurons to cutaneous itch input, the spinal cord was pretreated with aCSF or nalurafine (500 nM) for 20 min before the intradermal injection of compound 48/80.

Drug applications to ex vivo preparations

To measure network-level activity evoked by itch-causing peptides, ligands were bath-applied to the spinal cord. Ligand concentrations were selected on the basis of those used in previous physiology experiments on ex vivo spinal cord samples (37, 51, 79). GRP (300 nM; Tocris, 1789) and octreotide (200 nM; Tocris, 1818) were applied for 3 and 7 min, respectively, and subsequent activity was recorded for 20 min. SP (1 μM; Sigma-Aldrich, S6883) was applied to the spinal cord for 3 min, and subsequent activity was recorded for 5 min. To determine whether neurons responded directly to itch-causing peptides and GPCR ligands used for pharmacological profiling, 500 nM TTX (Abcam, 120055) was applied to the spinal cord and allowed to circulate for 8 to 15 min to suppress network activity. Then, agonists were diluted in TTX and applied to the spinal cord for 3 min at the following concentrations: GRP, 300 nM; SP, 1 μM; neurokinin B (NKB), 500 nM (Tocris, 1582); taltirelin, 3 μM (Adooq Bioscience, A18250); oxytocin, 1 μM (Sigma-Aldrich, O4375); cholecystokinin, 200 nM (Tocris, 11661); and oxotremorine M, 50 μM (Tocris, 1067). The same experimental design was used to determine which GPCR ligands induce cell-intrinsic oscillations. In experiments examining the mechanism of GRP-induced Ca²⁺ oscillations, GRP was first applied to the spinal cord to evoke Ca²⁺ oscillations and 2-APB (100 μM; Tocris, 1224) was then applied 10 min later, followed by a second GRP application after another 10 min. In CPA experiments, the spinal cord was pretreated with CPA (10 μM; Tocris, 1235) for 10 min before the application of GRP and Ca²⁺ responses were recorded for 25 min thereafter. At the end of each experiment, a high K⁺ aCSF solution (30 mM KCl) was applied for ~45 s to confirm cell viability.

Image processing and data extraction

Recording files were prepared for image processing using macros in FIJI (ImageJ, NIH). Macros are available on github and archived

Zenodo (<https://doi.org/10.5281/zenodo.12005206>). Suite2p (HHMI Janelia) was used for image registration. Then, another ImageJ macro (<https://doi.org/10.5281/zenodo.12006552>) was used to review stabilized recordings, generate summary images of regions of interest (ROIs) for selection, and produce averages of the recordings to assist in refining ROIs. We preferred manually selecting ROIs as opposed to using suite2p-generated masks because of the heterogeneity of spinal neurons soma size left SPBNs undetected by suite2p. Only cells that had a stable XY location and were free of Z drift were included in analyses. Following ROI selection, FIJI was used to extract raw mean fluorescence intensity. Using either R or Python (Full Python analysis pipeline available on Zenodo: <https://doi.org/10.5281/zenodo.12011425>), the Δ*f/f* for each ROI was calculated using the following rolling ball baseline calculation: For each frame (*F_i*), the 20th percentile value of the surrounding 6.6 min of frames was used as a baseline (*F_b*) to perform the Δ*f/f* calculation [(*F_i*−*F_b*)/*F_b*]. Rolling ball normalization was applied to minimize effects of gradual photobleaching of GCaMP6s and/or minor changes in ROI location. Δ*f/f* values for each cell then were plotted over time, and traces were visually reviewed. ROIs with recordings that demonstrated Z drift, were unresponsive to high K⁺ application, or exhibited cell death over the course of the recording were omitted from analysis. Neurons demonstrating basal spontaneous activity were included in counts of total neurons recorded but were uninterpretable and thus excluded from analyses for responsiveness to itch-inducing neuropeptides or cutaneous stimuli.

Analysis of Ca²⁺ activity

For analyses of ongoing neuronal activity in response to itch-inducing peptides and compound 48/80, the area under the curve (AUC) of Ca²⁺ activity was calculated for each cell. To determine a response threshold, we first manually identified cells with a visually robust, sustained Ca²⁺ response from a dataset of ~750 neurons taken from multiple aCSF-treated preparations. A receiver operator characteristic analysis was then performed, and the AUC value with 95% specificity was selected to minimize inclusion of false positives. The average AUC threshold was determined by dividing the cumulative AUC threshold (i.e., the summed AUC of all activity following compound 48/80 injection) by the number of 2.5 min bins (GRP, octreotide, and compound 48/80) or 1 min bins (SP) in the recording. This corresponded to an average AUC of at least (0.462 s * Δ*f/f*)/bin relative to baseline activity. If cells met this AUC threshold, they were labeled as responders for a given stimulus.

For analyses categorizing neurons for convergent population analyses as well as responses to GPCR agonists, neurons were classified as binary responders (yes/no). Neurons were considered binary responders if they displayed a peak Ca²⁺ response within 60 s of applying pharmacological stimuli with an increase in Δ*f/f* that was both ≥30% and ≥5 SDs of baseline activity in the 30 s preceding stimulus application. The response window was chosen to account for variability in time required for different drugs to penetrate the spinal cord and their subsequent activation of intracellular signaling cascades.

For analyses categorizing SPBNs as responsive to mechanical stimuli, neurons were considered responsive to noxious mechanical input if either application of a 2.0-g von Frey filament anywhere within their receptive field or a needle injection evoked a Ca²⁺

response. Neurons were considered responsive to dynamic light brush if brushing of the skin elicited a Ca^{2+} response in at least two of three applications. For each mechanical stimulus, neurons were considered binary responders if they displayed an increase in $\Delta f/f$ that was both $\geq 30\%$ and ≥ 5 SDs of baseline activity in the 30 s preceding the first stimulus application of the series). Using previously published criteria (80), we further categorized SPBNs as LT, HT, or WDR based on their response to these mechanical stimuli. Briefly, LT neurons were equally responsive to low-threshold (i.e., dynamic light brush) and noxious input (i.e., 2.0-g von Frey filament and needle injection), HT neurons were activated exclusively by noxious input, and WDR neurons were more strongly activated by noxious input than low-threshold input.

Behavior

All behavior experiments were conducted on mice from a C57BL/6J background. Behavior was conducted in a designated, temperature-controlled room, with the experimenter blinded to treatment to minimize bias. Injection sites were shaved at least 24 hours before testing. All behavior experiments were performed during the light cycle between 9 a.m. and 6 p.m.

On the day of testing, the mice were allotted 30 min to acclimate to a Plexiglas chamber on an elevated platform. Behavior platforms had a translucent glass surface, enabling bottom-up recording of animals using a Sony HD Camera (HDR-CX405). The experimenter left the behavior room once the last animal was injected. Behavior was later scored by an observer blind to treatment. Only the mice that were successfully injected were included in data analysis.

Intrathecal neuropeptide-evoked scratching

Itch peptides were administered intrathecally to awake, behaving mice. The mice were pinned by their pelvic girdle, and a 25- μl Hamilton syringe with a 30-G needle attachment was inserted between the L5 and L6 vertebrae. Successful targeting of the intervertebral space was demonstrated by a sudden involuntary lateral tail movement. A total of 5 μl of drug was injected at a rate of 1 $\mu\text{l}/\text{s}$, and the needle was held in place for 5 s before removal to minimize backflow. The following peptides were delivered in 5 μl of sterile saline: GRP (295 ng; Tocris, 1789), SP (400 ng; Sigma-Aldrich, S6883), octreotide (30 ng; Tocris, 1818), and GR 73632 (40 ng; Tocris, 1669). Immediately following injection, the mice were returned to their Plexiglas behavior chambers and recorded for 5 to 20 min. In studies with KOR agonists, 4% dimethyl sulfoxide (DMSO) in sterile saline was used as a vehicle, and itch peptides were either administered alone or coadministered with nalfurafine (40 ng). Immediately following the injection, the mice were returned to their individual Plexiglas chamber and were recorded for 30 min.

Intradermal pruritogen-evoked scratching

Mice were pretreated with either vehicle (4% DMSO) or nalfurafine (40 ng in 5 μl). Twenty minutes later, a 25- μl Hamilton syringe with a 30-G needle attachment was used to deliver either chloroquine (100 μg in 10 μl ; Sigma-Aldrich, C6628) or compound 48/80 (91 μg in 10 μl ; Sigma-Aldrich, C2313) intradermally in the nape of the neck. A successful intradermal injection was indicated by the appearance of a bleb at the injection site. Following the injection, the mice were returned to their Plexiglas behavior chambers and recorded for 30 min.

RNAscope FISH

The animals were anesthetized with isoflurane and quickly decapitated. The L3-L5 spinal cord segments were rapidly removed and flash frozen, and 15- μm sections were directly mounted onto Superfrost Plus slides. FISH experiments were performed according to the manufacturer's instructions for fresh frozen samples (Advanced Cell Diagnostics, 320293 or 323100). Briefly, spinal cord sections were fixed in ice-cold 4% paraformaldehyde for 15 min, dehydrated in ethanol, permeabilized at room temperature with protease for 15 min, and hybridized at 40°C with gene-specific probes to mouse, including the following: *Grpr* (#317871), *Tacr1* (#428781), *Cre* (#474001), *Tac1* (#410351), *Grp* (#317861), *Slc17a6* (#456751), *Egfp* (#400281), and *Oprk1* (#316111). Hybridized probe signal was then amplified and fluorescently labeled. Slides were mounted with Prolong Gold with 4',6-diamidino-2-phenylindole (DAPI) to visualize nuclei.

Intraspinal injections

Intraspinal viral injections were performed on 5- to 7-week-old mice. The animals were anesthetized with a ketamine (95 mg/kg)/xylazine (4.8 mg/kg)/acepromazine (0.95 mg/kg) cocktail. They were then prepared for surgery: The back was shaved, local antiseptic (betadine and ethanol) was applied to the skin, and a scalpel was used to make an incision over the T12-L3 vertebrae. Muscle and fascia were removed, exposing the L3/L4 and L4/L5 spinal segments. For each segment, a glass capillary filled with virus was lowered 300 μm below the surface of the spinal cord to target the dorsal horn, and a Nanoinject III was used to deliver 500 nl of virus at 5 nl/s. The glass capillary was left in place for 5 min following each injection and slowly withdrawn. The skin was sutured closed with 6-0 vicryl suture. For postoperative care, the mice were injected with ketofen (5 mg/kg) and buprenorphine (0.03 mg/kg) and allowed to recover on a heating pad. Histology experiments began at least 4 weeks following viral injection to allow sufficient time for the viral labeling to reach the brain.

Immunohistochemistry

For histology studies visualizing the central projection of spinal output neurons, the mice were anesthetized with intraperitoneal injection urethane (4 mg/kg, i.p.) and transcardially perfused with 4% paraformaldehyde. Spinal cord and brain were removed and post-fixed in 4% paraformaldehyde for either 2 hours (spinal cord) or overnight (brain). Tissues were then washed in phosphate-buffered saline (PBS), sunk in 30% sucrose, and cryosectioned at either 20 μm (spinal cord) or 40 μm (brain). The sections were incubated in a blocking solution made of 10% donkey serum (Jackson ImmunoResearch, 017-000-121) and 0.3% Triton X-100 in PBS (PBS-T) for 1 hour at room temperature. The sections were incubated overnight at 4°C with the primary antibody rabbit anti-red fluorescent protein (RFP, Rockland, 600-401-379) diluted at 1:1 K in an antibody buffer consisting of 5% donkey serum and (PBS-T). Following washes in PBS-T, the sections were incubated for 1 hour at room temperature with the secondary antibody donkey anti-rabbit Alexa Fluor 555 (Invitrogen, A-31572) at 1:500 diluted in antibody buffer. Tissues were washed in PBS and mounted with Prolong Gold with DAPI (Invitrogen, P36931).

Image acquisition and quantification

Full-thickness tissue sections were imaged using an upright epifluorescent microscope (Olympus BX53 with UPlanSApo 4 \times , 10 \times , or

20× objective) or confocal microscope (Nikon A1R with a 20× oil-immersion objective). Image analysis was performed off-line using FIJI imaging software (ImageJ, NIH). In FISH experiments evaluating markers in superficial dorsal horn neurons, the superficial dorsal horn was defined as the region between the surface of the gray matter and the bottom of the substantia gelatinosa, a region ~65 μm thick corresponding to lamina I and II. For FISH experiments evaluating coexpression of *Oprk1* in spinal cord neuronal markers, three spinal cord hemisections were manually quantified from three to four mice per marker. For FISH experiments visualizing retrogradely labeled SPBNs, 9 to 15 hemisections per mouse were imaged to ensure that enough sparsely labeled projection neurons were available for analysis. In immunohistochemistry experiments assessing the central targets of *Grpr-Cre* and *Oprk1-Cre* spinal projection neurons, brain sections from three mice were imaged, and brain structures with mCherry/RFP signal were recorded.

Quantification, statistical analysis, and data visualization

Microsoft Excel, GraphPad Prism, EulerAPE (81), R, and Python packages including Scipy, numpy, pandas, matplotlib, and other custom codes were used for data organization, processing, visualization, and statistical analyses. Log-linear analyses were used to test whether populations of neurons overlap more than expected by chance. Differences between mice were adjusted for using a mixed-effect model (i.e., a random intercept for mouse) when data were available for at least six mice. Otherwise, models included fixed-effects to adjust for the effect of each mouse. Analyses of neuronal responses to GPCR agonists were run as logistic (i.e., compound 48/80 binary responder) and linear (AUC) regressions, adjusting for mouse as fixed-effects. Linear mixed-effect model analyses were used to examine the effect of nalurfafine on Ca^{2+} responses. To reduce the influence of outliers, AUC values were winsorized to 3 SDs and log transformed, and differences between mice were adjusted for using a random intercept for mouse.

Throughout the figures, statistical significance is indicated with the following symbols: * $P < 0.05$, ** $P < 0.01$, *** $P < 0.001$, **** $P < 0.0001$, ^^^ $P < 1 \times 10^{-8}$, and ^^^^ $P < 1 \times 10^{-10}$. A Bonferroni correction was used to correct for multiple comparisons when appropriate. Experiment-specific details can be found in the figure legends. Data are presented as means \pm SEM, with a few exceptions. Where applicable, open circles are used to represent individual mice. Odds ratio analyses are presented as the odds ratio estimate \pm upper and lower 95% confidence interval (CI). Linear regression analyses are presented as estimate \pm upper and lower 95% CI. Representative traces of the Ca^{2+} responses of populations of neurons are presented as either median \pm interquartile range or mean and 10th through 90th percentile. For experiments in which GPCR ligands were used to characterize compound 48/80-responsive neurons or test for cell-intrinsic oscillations, the percentage of activated neurons adds up to more than 100% because many neurons responded to multiple ligands. When showing responses of compound 48/80-responsive neurons to GPCR ligands, each cell's trace was normalized to a maximum of 1 and a minimum of 0.

Supplementary Materials

This PDF file includes:

Figs. S1 to S10

REFERENCES AND NOTES

1. Y. G. Sun, Z.-F. Chen, A gastrin-releasing peptide receptor mediates the itch sensation in the spinal cord. *Nature* **448**, 700–703 (2007).
2. A. P. Kardon, E. Polgár, J. Hachisuka, L. M. Snyder, D. Cameron, S. Savage, X. Cai, S. Karnup, C. R. Fan, G. M. Hemenway, C. S. Bernard, E. S. Schwartz, H. Nagase, C. Schwarzer, M. Watanabe, T. Furuta, T. Kaneko, H. R. Koerber, A. J. Todd, S. E. Ross, Dynorphin acts as a neuromodulator to inhibit itch in the dorsal horn of the spinal cord. *Neuron* **82**, 573–586 (2014).
3. D. D. Sukhtankar, M.-C. Ko, Physiological function of gastrin-releasing peptide and neuromedin b receptors in regulating itch scratching behavior in the spinal cord of mice. *PLOS ONE* **8**, e67422 (2013).
4. T. D. Sheahan, C. A. Warwick, L. G. Fanien, S. E. Ross, The neurokinin-1 receptor is expressed with gastrin-releasing peptide receptor in spinal interneurons and modulates itch. *J. Neurosci.* **40**, 8816–8830 (2020).
5. J. Huang, E. Polgár, H. J. Solinski, S. K. Mishra, P.-Y. Tseng, N. Iwagaki, K. A. Boyle, A. C. Dickie, M. C. Kriegbaum, H. Wildner, H. U. Zeilhofer, M. Watanabe, J. S. Riddell, A. J. Todd, M. A. Hoon, Circuit dissection of the role of somatostatin in itch and pain. *Nat. Neurosci.* **21**, 707–716 (2018).
6. C. Ruzza, A. Rizzi, D. Malfacini, M. C. Cerlesi, F. Ferrari, E. Marzola, C. Ambrosio, C. Gro, S. Severo, T. Costa, G. Calo, R. Guerrini, Pharmacological characterization of tachykinin tetrabranch derivatives. *Br. J. Pharmacol.* **171**, 4125–4137 (2014).
7. J. L. K. Hylden, G. L. Wilcox, Intrathecal substance P elicits a caudally-directed biting and scratching behavior in mice. *Brain Res.* **217**, 212–215 (1981).
8. R. Gamse, A. Saria, Nociceptive behavior after intrathecal injections of substance P, neurokinin A and calcitonin gene-related peptide in mice. *Neurosci. Lett.* **70**, 143–147 (1986).
9. V. S. Seybold, J. L. K. Hylden, G. L. Wilcox, Intrathecal substance P and somatostatin in rats: Behaviors indicative of sensation. *Peptides* **3**, 49–54 (1982).
10. M. Häring, A. Zeisel, H. Hochgerner, P. Rinwa, J. E. T. Jakobsson, P. Lönnerberg, G. La Manno, N. Sharma, L. Borgius, O. Kiehn, M. C. Lagerström, S. Linnarsson, P. Ernfors, Neuronal atlas of the dorsal horn defines its architecture and links sensory input to transcriptional cell types. *Nat. Neurosci.* **21**, 869–880 (2018).
11. A. J. Todd, R. C. Spike, E. Polgár, A quantitative study of neurons which express neurokinin-1 or somatostatin sst2a receptor in rat spinal dorsal horn. *Neuroscience* **85**, 459–473 (1998).
12. N. A. Jansen, G. J. Giesler Jr., Response characteristics of pruriceptive and nociceptive trigeminoparabrachial tract neurons in the rat. *J. Neurophysiol.* **113**, 58–70 (2015).
13. T. Akiyama, E. Curtis, T. Nguyen, M. I. Carstens, E. Carstens, Anatomical evidence of pruriceptive trigeminohalamic and trigeminoparabrachial projection neurons in mice. *J. Comp. Neurol.* **524**, 244–256 (2016).
14. R. Wercberger, J. M. Braz, J. A. Weinrich, A. I. Basbaum, Pain and itch processing by subpopulations of molecularly diverse spinal and trigeminal projection neurons. *Proc. Natl. Acad. Sci. U.S.A.* **118**, e2105732118 (2021).
15. S. Davidson, X. Zhang, C. H. Yoon, S. G. Khasabov, D. A. Simone, G. J. Giesler, The itch-producing agents histamine and cowhage activate separate populations of primate spinothalamic tract neurons. *J. Neurosci.* **27**, 10007–10014 (2007).
16. S. Davidson, X. Zhang, S. G. Khasabov, H. R. Moser, C. N. Honda, D. A. Simone, G. J. Giesler, Pruriceptive spinothalamic tract neurons: Physiological properties and projection targets in the primate. *J. Neurophysiol.* **108**, 1711–1723 (2012).
17. D. Piyush Shah, A. Barik, The spino-parabrachial pathway for itch. *Front. Neural Circuits* **16**, 805831 (2022).
18. H. R. Moser, G. J. Giesler Jr., Characterization of pruriceptive trigeminohalamic tract neurons in rats. *J. Neurophysiol.* **111**, 1574–1589 (2014).
19. X. Ren, S. Liu, A. Virlogeux, S. J. Kang, J. Brusck, Y. Liu, S. M. Dymecki, S. Han, M. Goulding, D. Acton, Identification of an essential spinoparabrachial pathway for mechanical itch. *Neuron* **111**, 1812–1829.e6 (2023).
20. T. Akiyama, T. Nguyen, E. Curtis, K. Nishida, J. Devireddy, J. Delahanty, M. I. Carstens, E. Carstens, A central role for spinal dorsal horn neurons that express neurokinin-1 receptors in chronic itch. *Pain* **156**, 1240–1246 (2015).
21. D. Cameron, E. Polgár, M. Gutierrez-Mecinas, M. Gomez-Lima, M. Watanabe, A. J. Todd, The organisation of spinoparabrachial neurons in the mouse. *Pain* **156**, 2061–2071 (2015).
22. S. Choi, J. Hachisuka, M. A. Brett, A. R. Magee, Y. Omori, N.-A. Iqbal, D. Zhang, M. M. DeLisle, R. L. Wolfson, L. Bai, C. Santiago, S. Gong, M. Goulding, N. Heintz, H. R. Koerber, S. E. Ross, D. D. Ginty, Parallel ascending spinal pathways for affective touch and pain. *Nature* **587**, 258–263 (2020).
23. S. Inan, A. Cowan, Antipruritic effects of Kappa opioid receptor agonists: Evidence from rodents to humans in *The Kappa Opioid Receptor. Handbook of Experimental Pharmacology*, L.-Y. Liu-Chen, S. Inan, Eds. (Springer International Publishing, 2022), pp. 275–292.
24. B. S. Kim, The translational revolution of itch. *Neuron* **110**, 2209–2214 (2022).

25. T. Akiyama, M. I. Carstens, D. Piecha, S. Steppan, E. Carstens, Nalfurafine suppresses pruritogen- and touch-evoked scratching behavior in models of acute and chronic itch in mice. *Acta Derm. Venereol.* **95**, 147–150 (2015).
26. M.-C. Ko, S. M. Husbands, Effects of atypical κ -opioid receptor agonists on intrathecal morphine-induced itch and analgesia in primates. *J. Pharmacol. Exp. Ther.* **328**, 193–200 (2009).
27. E. Nguyen, G. Lim, H. Ding, J. Hachisuka, M.-C. Ko, S. E. Ross, Morphine acts on spinal dynorphin neurons to cause itch through disinhibition. *Sci. Transl. Med.* **13**, eabc3774 (2021).
28. E. Polgár, A. C. Dickie, M. Gutierrez-Mecinas, A. M. Bell, K. A. Boyle, R. Quillet, E. A. Rashid, R. A. Clark, M. T. German, M. Watanabe, J. S. Riddell, A. J. Todd, Grpr expression defines a population of superficial dorsal horn vertical cells that have a role in both itch and pain. *Pain* **164**, 149–170 (2023).
29. Z.-Q. Zhao, L. Wan, X.-Y. Liu, F.-Q. Huo, H. Li, D. M. Barry, S. Krieger, S. Kim, Z.-C. Liu, J. Xu, B. E. Rogers, Y.-Q. Li, Z.-F. Chen, Cross-inhibition of NMBR and GRPR signaling maintains normal histaminergic itch transmission. *J. Neurosci.* **34**, 12402–12414 (2014).
30. B. Aresh, F. B. Freitag, S. Perry, E. Blümel, J. Lau, M. C. M. Franck, M. C. Lagerström, Spinal cord interneurons expressing the gastrin-releasing peptide receptor convey itch through VGLUT2-mediated signaling. *Pain* **158**, 945–961 (2017).
31. F. B. Freitag, A. Ahemaiti, J. E. T. Jakobsson, H. M. Weman, M. C. Lagerström, Spinal gastrin releasing peptide receptor expressing interneurons are controlled by local phasic and tonic inhibition. *Sci. Rep.* **9**, 16573 (2019).
32. E. Polgár, C. Durrieux, D. I. Hughes, A. J. Todd, A quantitative study of inhibitory interneurons in laminae I–III of the mouse spinal dorsal horn. *PLOS ONE* **8**, e78309 (2013).
33. T. Yasaka, S. Y. X. Tiong, D. I. Hughes, J. S. Riddell, A. J. Todd, Populations of inhibitory and excitatory interneurons in lamina II of the adult rat spinal dorsal horn revealed by a combined electrophysiological and anatomical approach. *Pain* **151**, 475–488 (2010).
34. P. W. Mantyh, E. DeMaster, A. Malhotra, J. R. Ghilardi, S. D. Rogers, C. R. Mantyh, H. Liu, A. I. Basbaum, S. R. Vigna, J. Maggio, D. A. Simone, Receptor endocytosis and dendrite reshaping in spinal neurons after somatosensory stimulation. *Science* **268**, 1629–1632 (1995).
35. X. Wang, J. Marvizón, Time-course of the internalization and recycling of neurokinin 1 receptors in rat dorsal horn neurons. *Brain Res.* **944**, 239–247 (2002).
36. H. Wang, H. S. Wang, Z. P. Liu, Agents that induce pseudo-allergic reaction. *Drug Discov. Ther.* **5**, 211–219 (2011).
37. C. Warwick, J. Salsovic, J. Hachisuka, K. M. Smith, T. D. Sheahan, H. Chen, J. Ibinson, H. R. Koerber, S. E. Ross, Cell type-specific calcium imaging of central sensitization in mouse dorsal horn. *Nat. Commun.* **13**, 5199 (2022).
38. J. Hachisuka, H. R. Koerber, S. E. Ross, Selective-cold output through a distinct subset of lamina I spinoparabrachial neurons. *Pain* **161**, 185–194 (2020).
39. R. Bardoni, K.-F. Shen, H. Li, J. Jeffrey, D. M. Barry, A. Comitato, Y.-Q. Li, Z.-F. Chen, Pain inhibits GRPR neurons via GABAergic signaling in the spinal cord. *Sci. Rep.* **9**, 15804 (2019).
40. A. Munanairi, X.-Y. Liu, D. M. Barry, Q. Yang, J.-B. Yin, H. Jin, H. Li, Q.-T. Meng, J.-H. Peng, Z.-Y. Wu, J. Yin, X.-Y. Zhou, L. Wan, P. Mo, S. Kim, F.-Q. Huo, J. Jeffrey, Y.-Q. Li, R. Bardoni, M. R. Bruchas, Z.-F. Chen, Non-canonical opioid signaling inhibits itch transmission in the spinal cord of mice. *Cell Rep.* **23**, 866–877 (2018).
41. D. E. Russ, R. B. P. Cross, L. Li, S. C. Koch, K. J. E. Matson, A. Yadav, M. R. Alkassasi, D. I. Lee, C. E. Le Pichon, V. Menon, A. J. Levine, A harmonized atlas of mouse spinal cord cell types and their spatial organization. *Nat. Commun.* **12**, 5722 (2021).
42. A. Zeisel, H. Hochgerner, P. Lönnerberg, A. Johnsson, F. Memic, J. van der Zwan, M. Häring, E. Braun, L. E. Borm, G. La Manno, S. Codeluppi, A. Furlan, K. Lee, N. Skene, K. D. Harris, J. Hjerling-Lefler, E. Arenas, P. Ernfors, U. Marklund, S. Linnarsson, Molecular architecture of the mouse nervous system. *Cell* **174**, 999–1014.e22 (2018).
43. J. R. Sanders, B. Ashley, A. Moon, T. E. Woolley, K. Swann, PLC ζ Induced Ca²⁺ oscillations in mouse eggs involve a positive feedback cycle of Ca²⁺ induced InsP₃ formation from cytoplasmic PIP₂. *Front. Cell Dev. Biol.* **6**, 36 (2018).
44. M. Nomikos, J. Kashir, K. Swann, F. A. Lai, Sperm PLC ζ : From structure to Ca²⁺ oscillations, egg activation and therapeutic potential. *FEBS Lett.* **587**, 3609–3616 (2013).
45. R. Thul, Translating intracellular calcium signaling into models. *Cold Spring Harb. Protoc.* **2014**, pdb.top066266 (2014).
46. T. Oikawa, Y. Kuroda, K. Matsuo, Regulation of osteoclasts by membrane-derived lipid mediators. *Cell. Mol. Life Sci.* **70**, 3341–3353 (2013).
47. S. Zhang, N. Fritz, C. Ibarra, P. Uhlén, Inositol 1,4,5-trisphosphate receptor subtype-specific regulation of calcium oscillations. *Neurochem. Res.* **36**, 1175–1185 (2011).
48. T. Matsu-Ura, H. Shirakawa, K. G. N. Suzuki, A. Miyamoto, T. Michikawa, A. Kusumi, K. Mikoshiba, Dual-FRET imaging of IP₃ and Ca²⁺ revealed Ca²⁺-induced IP₃ production maintains long lasting Ca²⁺ oscillations in fertilized mouse eggs. *Sci. Rep.* **9**, 4829 (2019).
49. Y.-G. Sun, Z.-Q. Zhao, X.-L. Meng, J. Yin, X.-Y. Liu, Z.-F. Chen, Cellular basis of itch sensation. *Science* **325**, 1531–1534 (2009).
50. D. Acton, X. Ren, S. Di Costanzo, A. Dalet, S. Bourane, I. Bertocchi, C. Eva, M. Goulding, Spinal neuropeptide Y1 receptor-expressing neurons form an essential excitatory pathway for mechanical itch. *Cell Rep.* **28**, 625–639.e6 (2019).
51. M. Pagani, G. W. Albigsetti, N. Sivakumar, H. Wildner, M. Santello, H. C. Johannssen, H. U. Zeilhofer, How gastrin-releasing peptide opens the spinal gate for itch. *Neuron* **103**, 102–117.e5 (2019).
52. G. W. Albigsetti, M. Pagani, E. Platonova, L. Hösl, H. C. Johannssen, J.-M. Fritschy, H. Wildner, H. U. Zeilhofer, Dorsal horn gastrin-releasing peptide expressing neurons transmit spinal itch but not pain signals. *J. Neurosci. Off. J. Soc. Neurosci.* **39**, 2238–2250 (2019).
53. T. Akiyama, M. Tominaga, K. Takamori, M. I. Carstens, E. Carstens, Role of spinal bombesin-responsive neurons in nonhistaminergic itch. *J. Neurophysiol.* **112**, 2283–2289 (2014).
54. T.-J. S. Shi, Q. Xiang, M.-D. Zhang, S. Barde, Y. Kai-Larsen, K. Fried, A. Josephson, L. Glüek, S. M. Deyev, A. V. Zvyagin, S. Schulz, T. Hökfelt, Somatostatin and its 2A receptor in dorsal root ganglia and dorsal horn of mouse and human: Expression, trafficking and possible role in pain. *Mol. Pain* **10**, 12 (2014).
55. M. L. Nichols, B. J. Allen, S. D. Rogers, J. R. Ghilardi, P. Honore, N. M. Luger, M. P. Finke, J. Li, D. A. Lappi, D. A. Simone, P. W. Mantyh, Transmission of chronic nociception by spinal neurons expressing the substance P receptor. *Science* **286**, 1558–1561 (1999).
56. P. W. Mantyh, S. D. Rogers, P. Honore, B. J. Allen, J. R. Ghilardi, J. Li, R. S. Daughters, D. A. Lappi, R. G. Wiley, D. A. Simone, Inhibition of hyperalgesia by ablation of lamina I spinal neurons expressing the substance P receptor. *Science* **278**, 275–279 (1997).
57. A. Barik, A. Sathyamurthy, J. Thompson, M. Seltzer, A. Levine, A. Chesler, A spinoparabrachial circuit defined by Tacr1 expression drives pain. *eLife* **10**, e61135 (2021).
58. B. Duan, L. Cheng, S. Bourane, O. Britz, C. Padilla, L. Garcia-Campmany, M. Krashes, W. Knowlton, T. Velasquez, X. Ren, S. E. Ross, B. B. Lowell, Y. Wang, M. Goulding, Q. Ma, Identification of spinal circuits transmitting and gating mechanical pain. *Cell* **159**, 1417–1432 (2014).
59. K. S. Al Ghamdi, E. Polgár, A. J. Todd, Soma size distinguishes projection neurons from neurokinin 1 receptor-expressing interneurons in lamina I of the rat lumbar spinal dorsal horn. *Neuroscience* **164**, 1794–1804 (2009).
60. O. Cheunsuang, R. Morris, Spinal lamina I neurons that express neurokinin 1 receptors: Morphological analysis. *Neuroscience* **97**, 335–345 (2000).
61. Z.-F. Chen, A neuropeptide code for itch. *Nat. Rev. Neurosci.* **22**, 758–776 (2021).
62. F. Wang, B. S. Kim, Itch: A paradigm of neuroimmune crosstalk. *Immunity* **52**, 753–766 (2020).
63. C. Guo, H. Jiang, C.-C. Huang, F. Li, W. Olson, W. Yang, M. Fleming, G. Yu, G. Hoekel, W. Luo, Q. Liu, Pain and itch coding mechanisms of polymodal sensory neurons. *Cell Rep.* **42**, 113316 (2023).
64. A. N. van den Pol, Neuropeptide transmission in brain circuits. *Neuron* **76**, 98–115 (2012).
65. M. P. Nusbaum, D. M. Blitz, E. Marder, Functional consequences of neuropeptide and small-molecule co-transmission. *Nat. Rev. Neurosci.* **18**, 389–403 (2017).
66. M. Schley, R. Rukwied, J. Blunk, C. Menzer, C. Konrad, M. Dusch, M. Schmelz, J. Benrath, Mechano-insensitive nociceptors are sufficient to induce histamine-induced itch. *Acta Derm. Venereol.* **93**, 394–399 (2013).
67. L. M. Johaneck, R. A. Meyer, R. M. Friedman, K. W. Greenquist, B. Shim, J. Borzan, T. Hartke, R. H. LaMotte, M. Ringkamp, A role for polymodal C-fiber afferents in nonhistaminergic itch. *J. Neurosci.* **28**, 7659–7669 (2008).
68. R. Krahe, F. Gabbiani, Burst firing in sensory systems. *Nat. Rev. Neurosci.* **5**, 13–23 (2004).
69. F. Zeldenrust, W. J. Wadman, B. Englitz, Neural coding with bursts-current state and future perspectives. *Front. Comput. Neurosci.* **12**, 48 (2018).
70. H. Chen, I. H. Bleimeister, E. K. Nguyen, J. Li, A. Y. Cui, H. J. Stratton, K. M. Smith, M. L. Baccei, S. E. Ross, The functional and anatomical characterization of three spinal output pathways of the anterolateral tract. *Cell Rep.* **43**, 113829 (2024).
71. T. Maier, M. Güell, L. Serrano, Correlation of mRNA and protein in complex biological samples. *FEBS Lett.* **583**, 3966–3973 (2009).
72. Y. Liu, A. Beyer, R. Aebersold, On the dependency of cellular protein levels on mRNA abundance. *Cell* **165**, 535–550 (2016).
73. D. Mu, J. Deng, K.-F. Liu, Z.-Y. Wu, Y.-F. Shi, W.-M. Guo, Q.-Q. Mao, X.-J. Liu, H. Li, Y.-G. Sun, A central neural circuit for itch sensation. *Science* **357**, 695–699 (2017).
74. L. M. Snyder, M. C. Chiang, E. Loeza-Alcocer, Y. Omori, J. Hachisuka, T. D. Sheahan, J. R. Gale, P. C. Adelman, E. I. Sypek, S. A. Fulton, R. L. Friedman, M. C. Wright, M. G. Duque, Y. S. Lee, Z. Hu, H. Huang, X. Cai, K. A. Meerschaert, V. Nagarajan, T. Hirai, G. Scherrer, D. H. Kaplan, F. Porreca, B. M. Davis, M. S. Gold, H. R. Koerber, S. E. Ross, Kappa opioid receptor distribution and function in primary afferents. *Neuron* **99**, 1274–1288.e6 (2018).
75. N. Sharma, K. Flaherty, K. Lezgiyeva, D. E. Wagner, A. M. Klein, D. D. Ginty, The emergence of transcriptional identity in somatosensory neurons. *Nature* **577**, 392–398 (2020).
76. K. Honda, M. Tominaga, F. Kusube, K. Takamori, Potential antipruritic neuronal targets of nalfurafine in the murine spinal dorsal horn. *Itch* **8**, e66 (2023).

77. Y. Zhou, K. Freeman, V. Setola, D. Cao, S. Kaski, M. J. Kreek, L.-Y. Liu-Chen, Preclinical studies on nalfurafine (TRK-820), a clinically used KOR agonist. *Handb. Exp. Pharmacol.* **271**, 137–162 (2022).
78. X. Cai, H. Huang, M. S. Kuzirian, L. M. Snyder, M. Matsushita, M. C. Lee, C. Ferguson, G. E. Homanics, A. L. Barth, S. E. Ross, Generation of a KOR-Cre knockin mouse strain to study cells involved in kappa opioid signaling. *Genesis* **54**, 29–37 (2016).
79. C. T. Pérez, R. H. Hill, S. Grillner, Substance P depolarizes lamprey spinal cord neurons by inhibiting background potassium channels. *PLOS ONE* **10**, e0133136 (2015).
80. D. A. Simone, L. S. Sorkin, U. Oh, J. M. Chung, C. Owens, R. H. LaMotte, W. D. Willis, Neurogenic hyperalgesia: Central neural correlates in responses of spinothalamic tract neurons. *J. Neurophysiol.* **66**, 228–246 (1991).
81. L. Micallef, P. Rodgers, eulerAPE: Drawing area-proportional 3-Venn diagrams using ellipses. *PLOS ONE* **9**, e101717 (2014).

Acknowledgments: We thank all members of the Ross laboratory for comments and suggestions, as well as M. C. Chiang and H. C. Chen for technical assistance. **Funding:** This work was supported by the following funding sources from the National Institutes of Health: F32NS110155 (T.D.S.), K99NS126569 (T.D.S.), RM1NS128775 (H.R.K.), R01NS096705 (H.R.K. and S.E.R.), and R01AR063772 (S.E.R.). **Author contributions:** Conceptualization: T.D.S., C.A.W., E.K.N., H.R.K., and S.E.R. Data curation: C.A.W., A.Y.C., and A.P.M. Methodology: C.A.W.,

H.R.K., and S.E.R. Formal analysis: T.D.S., C.A.W., A.Y.C., D.A.A.B., V.J.P., K.M.S., and A.P.M. Funding acquisition: T.D.S., H.R.K., and S.E.R. Resources: T.D.S., H.R.K., and S.E.R. Investigation: T.D.S., C.A.W., A.Y.C., V.J.P., A.P.M., E.K.N., and K.M.S. Validation: T.D.S., C.A.W., V.J.P., K.M.S., A.P.M., H.R.K., and S.E.R. Project administration: T.D.S., C.A.W., and S.E.R. Software: T.D.S., C.A.W., A.Y.C., and D.A.A.B. Supervision: T.D.S., C.A.W., H.R.K., and S.E.R. Visualization: T.D.S., C.A.W., A.Y.C., V.J.P., A.P.M., E.K.N., and K.M.S. Writing—original draft: T.D.S., C.A.W., V.J.P., and S.E.R. Writing—review and editing: T.D.S., C.A.W., A.Y.C., D.A.A.B., V.J.P., K.M.S., A.P.M., H.R.K., and S.E.R. **Competing interests:** The authors declare that they have no competing interests. **Data and materials availability:** All data needed to evaluate the conclusions in the paper are present in the paper and/or the Supplementary Materials. Packages for 2P image processing and data processing are available on GitHub and have been archived on Zenodo: ThorStackSplitter, <https://doi.org/10.5281/zenodo.12005206>; Suite2p-Output-Processor, <https://doi.org/10.5281/zenodo.12006552>; CalciumImagingAnalysis, <https://doi.org/10.5281/zenodo.12011425> (see Materials and Methods for a description of specific packages).

Submitted 3 April 2024
Accepted 20 August 2024
Published 25 September 2024
10.1126/sciadv.adp6038